Transportation Infrastructure Geotechnology
https://doi.org/10.1007/s40515-024-00417-3

TECHNICAL PAPER

Cumulative Liquefaction Susceptibility Index to Estimate Integrated Liquefaction at Bengkulu City, Indonesia

Lindung Zalbuin Mase[1]

Accepted: 16 May 2024

Abstract
Teluk Segara and Sungai Serut in Bengkulu City are significantly developed districts. This paper presents a liquefaction vulnerability map for the housing areas. The geophysical and geotechnical data for the study area are collected. A semi-empirical analysis is performed to estimate the liquefaction potential. The liquefaction potential index is estimated. The maps describing geophysical characteristics, liquefaction, and seismic vulnerabilities are discussed. The results showed that the study area could undergo moderate to strong motion during the most significant earthquake in Bengkulu City. It can trigger liquefaction in areas near the river dominated by sandy soils. The integrated weighted factor method, called the cumulative liquefaction susceptibility (CLSI), is proposed to estimate the level of liquefaction susceptibility. The factor considered several parameters such as liquefaction potential index, peak ground acceleration, seismic vulnerability, and site classification. The result shows that the study area is characterised as moderate liquefaction susceptibility. The integrated method can be implemented to understand liquefaction quantification in engineering practice better.

Keyword Liquefaction potential · Liquefaction vulnerability · Housing areas · Peak ground acceleration

1 Introduction

As a developed city in Indonesia, Bengkulu City has gradually improved its quality. Within the last 10 years, the socio-economic aspects in Bengkulu City have significantly grown. A sector of life, such as housing areas, is also well-developed (Putrie et al. 2019). The demand for housing pushes the change of land-use policy

✉ Lindung Zalbuin Mase
lmase@unib.ac.id

[1] Department of Civil Engineering, Faculty of Engineering, University of Bengkulu, Bengkulu 38371, Indonesia

Published online: 12 June 2024

(Farid and Mase 2020). However, the development sometimes meets limitations in minimising geohazard's impact (Porter et al. 2019). In Bengkulu City, at least two strong earthquakes occurred within the last 50 years. Mase (2022) mentioned the 2000 Bengkulu-Enggano Earthquake with a magnitude of M_w 7.9 and the 2007 Bengkulu-Mentawai Earthquake with a magnitude of M_w 8.6. The damage due to the earthquake was massive. Structural and geotechnical damage, such as liquefaction, ground, and slope failures, were also found (Farid and Mase 2020; Hausler and Anderson 2007). In line with this condition, the importance of spatial development based on hazard mitigation should be enforced.

Mase et al. (2021a) conducted a study of local site investigation and simulated a ground response analysis for areas in the Muara Bangkahulu River. The passive and active measurements used microtremor measurement and multichannel analysis of surface waves (MASW) to measure shear wave velocity (V_s) are performed. Site classification and V_{s30} distributions based on Building Seismic Safety Council (BSSC 2020) are presented. Mase et al. (2021a) suggested that the western part of the study area heading to the coastline of Bengkulu is vulnerable to seismic impact because the soil resistance is relatively low, and the groundwater level is generally found at a shallow depth. Mase et al. (2024a) also mentioned that the downstream area of Muara Bangkahulu River has a shallow to medium depth of engineering bedrock surface, which is also dominated by sedimented materials such as gravelly soil near the ground surface. The characteristics of the materials are relatively loose with low shear wave velocity and could be vulnerable to liquefaction (Aytaş et al. 2023). Sukkarak et al. (2021) also mentioned that the environmental setting, such as groundwater level, density of sandy soils, and cyclic resistance, also control the liquefaction potential in an area. The characteristics of composed materials near the river with complex geological conditions deliver the understanding that liquefaction could happen under a seismic event, such as an earthquake. Mase (2017), Riveros et al. (Riveros and Sadrekarimi 2020), Wang et al. (2022), and Ansari et al. (Ansari et al. 2022) reported that liquefaction during earthquakes is found along the rivers. The characteristics of sedimented materials, with low shear resistance and under-saturated conditions, could be why liquefaction could happen in this area. In line with past studies, analysing liquefaction potential and mapping an area's vulnerability zone is important.

Several researchers have presented studies on liquefaction hazard maps. Sonmez (2003) analysed liquefaction based on the updated liquefaction potential index and susceptibility data for an earthquake-prone area called Inegol in Turkey. Sonmez and Gokceoglu (2005) proposed a hazard mapping method using the liquefaction susceptibility index or LSI to quantify liquefaction. The main parameter to analyse LSI is the probability of liquefaction (PL). Maurer et al. (2014) mapped the liquefaction potential index during the Christchurch Earthquake in 2011. Rahman et al. (2015) conducted a liquefaction hazard analysis and composed Dhaka City in Bangladesh's liquefaction potential index map. Kim et al. (2021) compared a method called liquefaction potential index or LPI and liquefaction severity number (LSN) in Pohang, Korea. Based on these previous studies, the LPI method is generally implemented to describe the liquefaction susceptibility. LPI itself is derived based on the simplified procedure method first to find the factor of safety (FS). FS is then analysed based on weighted factors and depth to quantify the level of liquefaction potential. Those

previous methods are generally performed based on a single parameter, i.e. FS and PL. So far, implementing the method is essential to support hazard mitigation in an area. However, the integrated method of mapping liquefaction. Other parameters contributing to determining liquefaction impacts, such as peak ground acceleration, seismic vulnerability, index of liquefaction, and site condition, are still rarely performed. Considering those parameters developed based on weighted factors, the integrated method is required to depict the general liquefaction susceptibility that covers all perspectives of contributed factors.

Quantifying liquefaction susceptibility should focus on several aspects, such as site characteristics, i.e. seismic vulnerability from geophysical measurement and site condition, external factors, i.e. peak ground acceleration, and liquefaction potential, i.e. index. So far, the quantification of liquefaction potential into one parameter that integrates those aspects has rarely been performed. In general, measuring liquefaction safety is still based on the factor of safety probability of liquefaction. Therefore, there is a need to present liquefaction susceptibility based on a parameter that integrates influencing factors. The result of the integrated method would provide a realistic liquefaction hazard map, which reflects the actual condition of a studied area. This study discusses a method to integrate all influencing parameters (CLSI).

This paper presents the analysis of liquefaction potential hazards in the study area. The site investigation data from previous studies, Mase et al. (2021a, 2024a), is used for the analysis. Estimating maximum peak ground acceleration (PGA) based on geophysical characteristics is performed. Liquefaction potential analysis using a simplified procedure is conducted. Furthermore, LPI is performed. The spatial mapping using the Kriging Interpolation Method is performed to depict the vulnerability zone of liquefaction. The integrated method based on weighted factors for affecting parameters is introduced in this study. This procedure is called the cumulative liquefaction susceptibility index or CLSI. The method is generally straightforward, considering the weighted value for contributed parameters. Using this method would deliver a better understanding of how to justify liquefaction susceptibility from the perspective of engineering practice. This study is expected to expose the liquefaction potential in the study area, which can be considered for developing a seismic hazard mitigation system.

2 Study Area and Seismotectonic Settings

2.1 Study Area

Figure 1 presents the study area layout. The zone along the river of Muara Bangkahulu in Bengkulu City is known as one of the developed areas in Bengkulu City, especially for housing purposes. This zone involves two central districts, the Sungai Serut District and the Teluk Segara District. Since the beginning of the 2000s, the population density growth in this area has been relatively high. Mase et al. (2021a, 2024a) and Farid and Mase (2020) suggested that this area is dominated by alluvium formation (Q_a) and alluvium terraces (Q_{at}) formed by floodplain materials with low to high density. Farid and Mase (2020) also mentioned that the seismic vulnerability

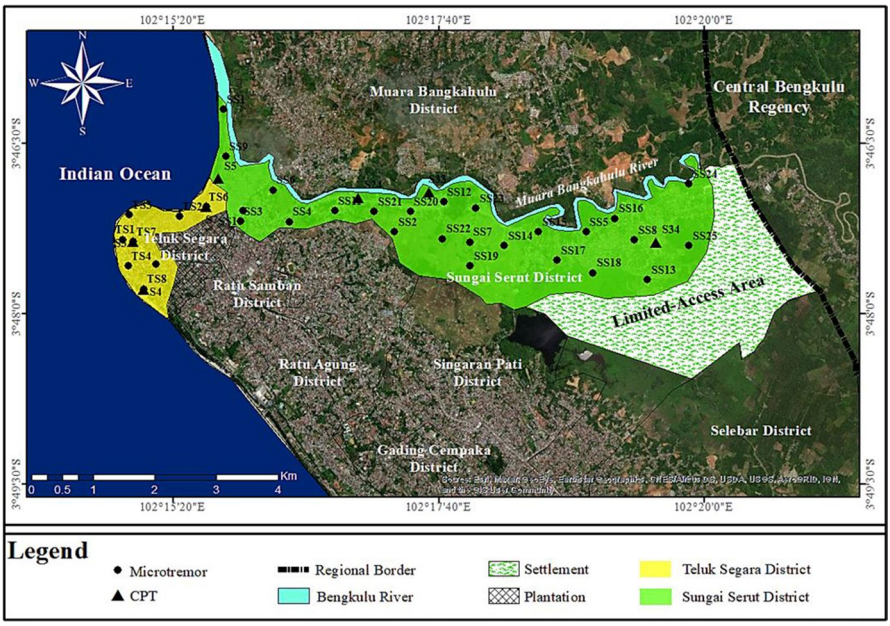

Fig. 1 Site investigation's locations

index (K_g) for areas along the river can be categorised as low to high seismic vulnerability, especially for areas following the river, which is dominated by thick, soft sediment thickness.

Most people living in the area are categorised as merchants, civil servants, sailors, etc. The variation of professions among the local people certainly influences the knowledge of natural hazards in this area. In addition, the position of the zone, which is located close to the river, can make this area very vulnerable to flooding hazards. Several local researchers have presented several studies on the impact of the Muara Bangkahulu River's inundation (Mase 2020a; Vatresia et al. 2023; Mase et al. 2022, 2023a). In general, those previous studies focused on the slope stability of river banks during floods. However, those previous studies had delivered a clue that the material composed of the area is from sedimented materials such as sand and loams. In addition, the groundwater level in the study area is also found at shallow depths. During a massive flood in 2019, all areas along the river had been inundated, which indicated that soils were under saturated conditions.

Mase et al. (2021a, 2024a) conducted a site investigation along the river. The black triangles indicate shallow site investigation by cone penetration test (CPT), and the black circles suggest the ambient noise measurement using a seismometer. Based on CPTs, the study area could have seven sandy layers at maximum. The first sand layer is dominated by poorly graded sand or SP with an average cone resistance (q_c) of about 3.668 MPa. Silty sand (SM) dominates the second sand layer with an average q_c of 6.89 MPa. SM and SP types are dominant for the third and fourth sand layers. Those layers have average q_c values of 9.249 MPa and 14.298 MPa,

respectively. Following those two layers, the fifth layer, dominated by clayey sand (SC), and the sixth layer, dominated by SP, have average q_c values of 12.554 MPa and 23.340 MPa, respectively. The seventh layer, dominated by SM, completes the ground profile based on CPT data, with an average q_c of about 28.684 MPa. An example of the ground profile in the study area can be seen in Fig. 2. From the figure, it can be observed that four sites were selected to represent the general characteristics of the study area. SS24 represents the upper hill of the study area. Housing areas and schools exist on this site. SS12 represents the small market zone in the study area where most people are centralised. SS9 represents the traditional zone where the first civilisation in Bengkulu City appeared. Those three sites are located in Sungai Serut Districts. Another site, TS7, is located in Teluk Segara District. This site represented the coastal area of the study area, where the traditional market, sailing activity, and old colonialism heritage exist. The soil profile and shear wave velocity (Vs) are presented for those figures.

Based on on-site investigation data presented in Fig. 2, it can be observed that the study area tends to be dominated by sandy soils. This seems reasonable because the study area is along the river where sedimented materials such as granular and alluvial soils are formed. There are also several types of sandy soils found in the study area, i.e. poor-graded sand (SP), silty sand (SM), and clayey sand (SC). The time-averaged shear wave velocity calculation for the first 30 m depth is also performed (V_{s30}). For the represented site, V_{s30} is observed to vary from 263.94 to 362.15 m/s. Those values ranges indicate sites are classified as Site Class C and Site Class D based on the Building Seismic Safety Council (BSSC 2020). In terms of groundwater level, the distribution of groundwater level in the study area is generally categorised as shallow groundwater level, i.e., about 0 to 1.5 m. This is because the study area, formed as a basin, is close to the river and coastline; therefore, the groundwater level distribution tends to follow the river water level. Bengkulu City is an earthquake-prone area, and under a site dominated by sandy soil with a shallow groundwater level, it seems ideal for sites to undergo liquefaction.

2.2 General Seismotectonic Settings

Bengkulu City, a city on the coastline of Sumatra Island, has been known as an earthquake-prone area. Figure 3 explains why the earthquake remains the central issue in Bengkulu City, especially for city development (Mase 2020). Several active tectonic settings are located near the city. The first is Sumatra Subduction, also known as the Sumatra Megathrust Zone (Rai et al. 2023). The subduction activity triggered some significant earthquakes along the west coastline of Sumatra Island. For Bengkulu City, two strong earthquakes in 2000 and 2007 occurred due to the activity of this subduction zone. Mase (Ambikapathy et al. 2010; Mase et al. 2024b) mentioned that the earthquake of 8.6 in 2007 was the most devastating in Bengkulu City. This earthquake, later known as the Bengkulu-Mentawai Earthquake, occurred in 2007. During this earthquake, liquefaction evidence was also reported by Hausler and Anderson (2007) and Mase et al. (2023b, 2024b).

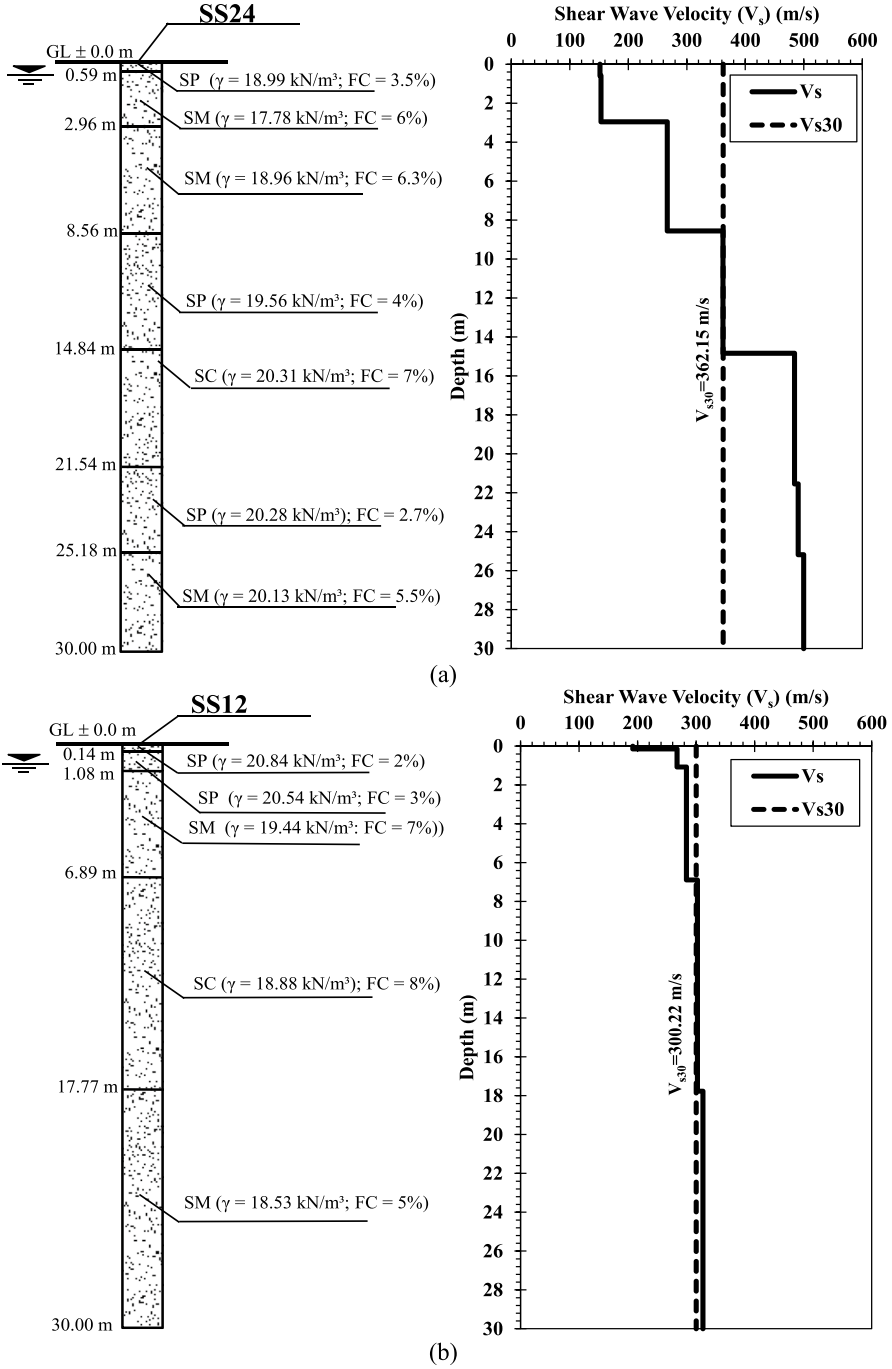

Fig. 2 Site investigation data in the study area for **a** SS24, **b** SS12, **c** SS9, and **d** TS7

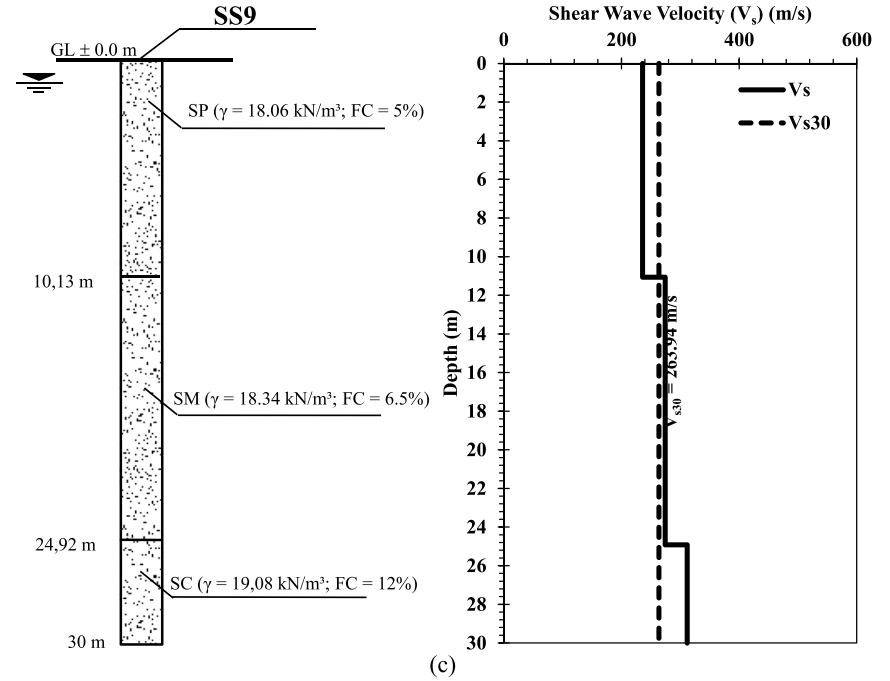

Fig. 2 (continued)

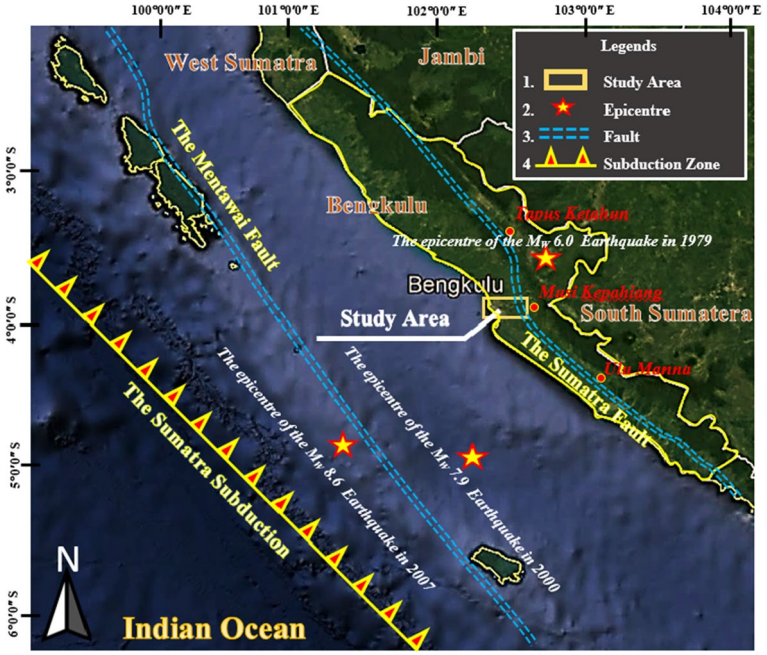

Fig. 3 General setting of seismotectonic condition in the Province of Bengkulu

On Sumatra Island, a tectonic fault called the Sumatra Fault also exists as the earthquake source (Rafie et al. 2023). For Bengkulu Province, three segments are parts of the fault. These segments are the Ketahun Segment, the Musi Segment, and the Manna Segment. The characteristics of earthquakes triggered under these active faults are generally shallow focal depth and low to moderate magnitude. The activity of this fault also triggered several earthquakes with moderate magnitude, such as the Liwa Earthquake in 1994 (Triyoso and Suwondo 2023). The position of these segments is relatively far from Bengkulu City, so the impact of the earthquake resulting from the earthquake produced under these segments is relatively insignificant.

Between the Sumatra Fault and Sumatra Subduction, the back-thrust fault system called the Mentawai Fault is located. This fault is located underneath the Indian Ocean. This fault triggered several significant earthquake events, such as the Padang Earthquake in 2009 (McCloskey et al. 2010). Since the position of this fault is in the Indian Ocean or similar to a megathrust system, the potential of tsunami waves produced after the earthquake is also high (Newman et al. 2011). Another earthquake event called the Mentawai Earthquake in 2010, and the tsunami waves climbed up to several meters, hitting areas in the Mentawai Archipelago.

3 Methodology

3.1 Liquefaction Potential Analysis

The simplified procedure method in liquefaction potential analysis has been well-developed. The main concept is to compare the driving and resisting parameters. Therefore, this procedure is also sometimes called the equilibrium method. The driving parameter describes the earthquake energy as the main factor triggering liquefaction, whereas the resisting parameter describes the potential strength characteristics provided by soil to retain from liquefaction (Ntritsos and Cubrinovski 2020).

The simplified procedure method's driving component is cyclic stress ratio or CSR. CSR reflects the cyclic stress produced by the maximum energy triggered by an earthquake, which is defined as maximum acceleration or PGA_{max}. The formulation to estimate this parameter by Idriss and Boulanger (Idriss and Boulanger 2006) is expressed in the following equation,

$$CSR = 0,65 r_d \left(\frac{PGA_{max}}{g}\right)\left(\frac{\sigma_v}{\sigma_v'}\right)\left(\frac{1}{K_\sigma}\right)\left(\frac{1}{MSF}\right) \tag{1}$$

where, CSR is cyclic stress ratio, PGA_{max} is maximum peak ground acceleration or PGA, σ_v is total stress and σ_v' is effective stress, g is gravitational excitation, K_σ is the correction of overburden pressure, r_d is depth reduction factor and MSF is magnitude scaling factor.

It should be noted that earthquake magnitude influences the amount of CSR; therefore, MSF is considered in the analysis using Eq. 1. For MSF, Idriss and Boulanger (2006) proposed the formulation, as expressed in the following equation:

$$MSF = 6,9\exp\left(\frac{-M_W}{4}\right) - 0,058 \leq 1,8 \tag{2}$$

According to Idriss and Boulanger (2006), the parameter of r_d is defined as a parameter depending on α and β. The formulation to estimate r_d is expressed in the following equations.

$$r_d = \exp[\alpha + \beta M_W] \tag{3}$$

$$\alpha = -1.012 - 1.126 \sin\left[5.133 + \left(\frac{z}{11.73}\right)\right] \tag{4}$$

$$\alpha = 0.106 + 0118 \sin\left[5.142 + \left(\frac{z}{11.28}\right)\right] \tag{5}$$

where z is the analysed depth, and M_w is the moment magnitude.

Boulanger and Idriss (2014) suggested that the overburden correction should be considered in the analysis. K_σ as the correction parameter for overburden pressure is defined in the following equations,

$$K_\sigma = 1 - C_\sigma \ln\left(\frac{\sigma'_v}{P_a}\right) \leq 1{,}1 \tag{6}$$

$$C_\sigma = \frac{1}{1.89 - 17.3\sqrt{\frac{\left(\frac{V_{s1}}{93.2}\right)^{\frac{1}{0.231}}}{46}}} \leq 0.3 \tag{7}$$

where P_a is the atmospheric pressure (about 100 kPa), and V_{s1} is the corrected V_s. Andrus et al. (2004) acknowledged that to estimate V_{s1}, parameters such as effective stress (σ'_{vo}), reference stress of 100 kPa (P_a), and the coefficient of earth pressure at rest (K'_o) should be considered in the analysis, as expressed in Eq. 8.

$$V_{s1} = V_s\left(\frac{P_a}{\sigma'_v}\right)^{0.25}\left(\frac{0.25}{K'_o}\right)^{0.125} \tag{8}$$

Also, in Eq. 1, in this study, classical mathematical modelling for estimating $PGA_{\max}$ is based on an attenuation model considering site characteristics suggested by Kanai's model (Douglas 2021),

$$PGA_{\max} = \frac{5}{\sqrt{T_0}} 10^{0.16M_w - (1.66 + \frac{3.6}{R})\log R + 0.167 - \frac{1.83}{R}} \tag{9}$$

PGA is peak ground acceleration, M_w is moment magnitude, T_0 is the predominant period estimated from the peak H/V curve, and R is hypocentre distance. It should be noted that T_0 for sites analysed in this study is collected based on previous studies of Mase et al. (2021a, 2024a).

CRR as cyclic resistance ratio is generated based on site investigation data. In this study, V_s data for each investigated site is used. The formulation of CRR is expressed in the following equation:

$$CRR = \{0.022\left(\frac{K_{a1}V_{s1}}{100}\right)^2 + 2.8\left(\frac{1}{V^*_{s1} - (K_{a1}V_{s1})} - \frac{1}{V^*_{s1}}\right)\}K_{a2} \tag{10}$$

K_{a1} and K_{a2} are ageing correction factors. Mase et al. (2021a) suggested that the downstream area of Bengkulu City is generally dominated by loose sedimented soils composed of Holocene alluvial deposits. Therefore, according to Andrus et al. (2004), both K_{a1} and K_{a2} can be justified to be set as one. Andrus and Stokoe (2000) suggested the upper-value limit for V_{s1}. This parameter is also related to finer percentage (FC), as expressed in the following equations:

$$V^*_{s1} = 215 \text{ m/s} \quad \text{for } FC \leq 5\% \tag{11}$$

$$V^*_{s1} = 215 - 0.5(FC - 5) \text{ m/s} \quad \text{for } 5\% < FC < 35\% \tag{12}$$

$$V_{s1}^{*} = 200 \text{ m/s} \text{ for } FC \geq 35\% \tag{13}$$

To obtain a site's severity condition from liquefaction, CRR and CSR are compared. The comparison of those parameters is known as the factor of safety (FS) against liquefaction, as expressed in Eq. 14. The sand layer is declared safe if FS is more than 1, whereas FS equal to 1 indicates the sand layer is under critical condition. FS less than 1 reflects an unsafe sand layer from liquefaction.

$$FS = \frac{CRR}{CSR} \tag{14}$$

3.2 Liquefaction Potential Index

The empirical method using a simplified procedure is addressed to estimate the safety condition of the sand layer to liquefaction. Nevertheless, the method cannot represent a whole site condition to liquefaction. In connection with this, the integrated method based on weighted factor consideration should be performed to depict the site condition under liquefaction. Several methods, such as the liquefaction potential index or LPI (Maurer et al. 2014; Iwasaki et al. 1984), liquefaction severity index or LSI (Sonmez 2003), and liquefaction severity number or LSN (Ballegooy et al. 2012), were widely used to depict liquefaction vulnerability. This study employs the updated version of the LPI method extended by Maurer et al. (2014).

Maurer et al. (2014) suggested that LPI is a weighted parameter representing the general liquefaction potential based on FS and depth. Equations 15 to 19 explained the mathematical procedure to estimate LPI:

$$LPI = \int_{0}^{20} Fw(z)dz \tag{15}$$

$$F = 1 - FS \text{ for } FS < 1 \tag{16}$$

$$F = 0 \text{ for } FS_{Liq} \geq 1 \tag{17}$$

$$w(z) = 10 - 0.5z \text{ for } 0 \leq \text{z} < 20 \text{ m} \tag{18}$$

$$w(z) = 0 \text{ for z} \geq 20 \text{ m} \tag{19}$$

To Iwasaki et al. (1984), an LPI less than five indicates low, an LPI between 5 and 15 indicates high, and an LPI more than 15 indicates very high. Maurer et al. (2014) and case study during the Christchurch Earthquake in 2011 in New Zealand modified the original LPI range based on Iwasaki et al. (1984). Maurer et al. (2014) classified the level of liquefaction potential to LPI less than four as no potential. LPI between 4 and 8 is marginal liquefaction, LPI between 8 and 15 has moderate potential, and LPI is more than 15, which is severe liquefaction potential.

3.3 MMI Level

Modified Mercalli Intensity (MMI) level (Wood and Newman 1931) is generally used to describe the potential seismic damage. MMI level can be predicted based on the maximum peak ground acceleration obtained from the analysis. Tjockrodimuljo (2000) and Mase (2020) suggested the formulation to estimate the MMI level based on the following equation:

$$\log(a_{\max}) = (\frac{1}{4}MMI) + \frac{1}{4} \tag{20}$$

3.4 The Cumulative Liquefaction Susceptibility Index (CLSI)

This study proposes a new quantification method to estimate liquefaction susceptibility. This method is namely the cumulative liquefaction susceptibility index (CLSI). The method is based on weighted factor analysis. Several parameters that contribute to determining the liquefaction are included to determine CLSI. PGA is selected as the contributed parameter. This is because PGA is the primary earthquake energy to produce soil and structural damage. V_{s30} is selected to represent site characteristics. Seismic vulnerability of K_g, estimated by the ratio between A0 square and f0, is selected as a fundamental parameter reflecting potential seismic impact. The last parameter, i.e. LPI, is selected to accomplish the integrated calculation and determine CLSI. CLSI is estimated based on the following equations:

$$CLSI = (W_{PGA} + W_{LPI} + W_{K_g} + W_{V_{s30}}) \tag{21}$$

where W_{PGA} is the weighted value for PGA, W_{LPI} is the weighted value for LPI, W_{K_g} is the weighted value for K_g, and $W_{V_{s30}}$ is the weighted value for V_{s30}. The maximum weighted value is 4, and the minimum one is 1.

W_{PGA} is estimated based on weighted values considered based on the PGA range. According to Kramer (1996), the minimum PGA of 0.1 g is used as the threshold of liquefaction. It is combined with the standard of strong motion, suggesting the criteria of motion strength (SNI 1726:2019). For weighted values, a PGA less than 0.1 g is given as 1, a PGA between 0.1 g and 0.17 g is given as 2, a PGA between 0.17 g and 0.53 g is given as 3, and a PGA more than 0.53 is given as 4.

W_{LPI} is estimated based on the classification of LPI suggested by Maurer et al. (2014). The LPI value is estimated using a semi-empirical procedure based on site investigation data. In the calculation of CLSI, the weighted value for LPI less than 4 is 1, and LPI between 4 and 8 is given as 2. For LPI within 8 to 15, the weighted value is 3. The weighted value for LPI more than 15 is given as 4.

W_{K_g} is estimated based on the seismic vulnerability index, which is based on Akkaya (2020) and could be divided into four levels. K_g less than 3 is a low seismic vulnerability, given the weighted value of 1. K_g falls within 3 to 5 as moderate seismic vulnerability and is given the weighted value of 2. The weighted value of 3 is

given for high seismic vulnerability or K_g within 5 to 10. K_g more than ten, defined as very high seismic vulnerability, is given the weighted value of 4.

Wills et al. (2015) and Hollender et al. (2018) suggested that low V_{s30} indicates a higher seismic risk. Therefore, a lower V_{s30} means a more prominent weighted factor. In terms of $W_{V_{s30}}$ The value is based on the site classification suggested by BSSC (2020). V_{s30} less than 180 m/s has a weighted value of 4. V_{s30} falls within the range of 180 m/s to 360 m/s and is given a weighted value of 3. V_{s30} falls within the range of 360 m/s to 760 m/s and is given the weighted value of 2. The weighted value for V_{s30} is more than 760 m/s, given a weighted value 1.

In general, the maximum value of CLSI that can be obtained is 16, and the minimum value of CLSI is 4. Within this gap, the classification of CLSI can be defined as three classes. CLSI within the range 4 to 8 reflects low susceptibility, CLSI within the range 8 to 12 reflects moderate susceptibility, and LSI within 12 to 16 reflects high susceptibility. The new proposed method is relatively simple and can cover the critical factors in determining liquefaction. This study implements the proposed method in the Muara Bangkahulu River area case study.

3.5 Analytical Framework

Figure 4 presents the analytical framework implemented in this study. This study was initiated by capturing the issues of earthquakes and liquefaction in Bengkulu City. The problem definition in this study is to propose a hazard map for liquefaction potential in the study area. Furthermore, the data collection is performed. Data including geophysical characteristics such as amplitude of horizontal to the vertical spectral ratio (*H/V*) or A_0, predominant frequency (f_0), and natural period (T_0) is collected. Ambikapathy et al. (2010) and Mase et al. (Mase 2020; Mase et al. 2023b) revealed that the M_w 8.6 Bengkulu-Mentawai Earthquake (epicentre shown in Fig. 3) is defined as the most controlling earthquake in Bengkulu City because the damage intensity level produced by this earthquake is about X in maximum. Therefore, this earthquake should be considered for structural design and seismic hazard assessment, especially for seismic hazard assessment and pre-disaster evaluation. In addition, site investigation data, including soil profile and shear wave velocity, is also collected.

The information, such as T_0, is then used as the input parameter to estimate the maximum peak ground acceleration in each investigated site, together with hypocentre distance (R), epicentral distance (d), and focal depth (h). A classical Kanai model is proposed and adopted in this study. The model's important parameter represents the site characteristics related to resonance during an earthquake, i.e. T_0 is used. In addition, the MMI level predicted based on PGA_{max} is also estimated in this study. Afterwards, the liquefaction potential analysis is performed to determine the safety factor. Using the weighted factor analysis in the framework of the liquefaction potential index, the level of liquefaction vulnerability in the study area can be depicted.

Afterwards, a new method called cumulative liquefaction susceptibility index or CLSI is proposed to depict a general description of liquefaction susceptibility in the

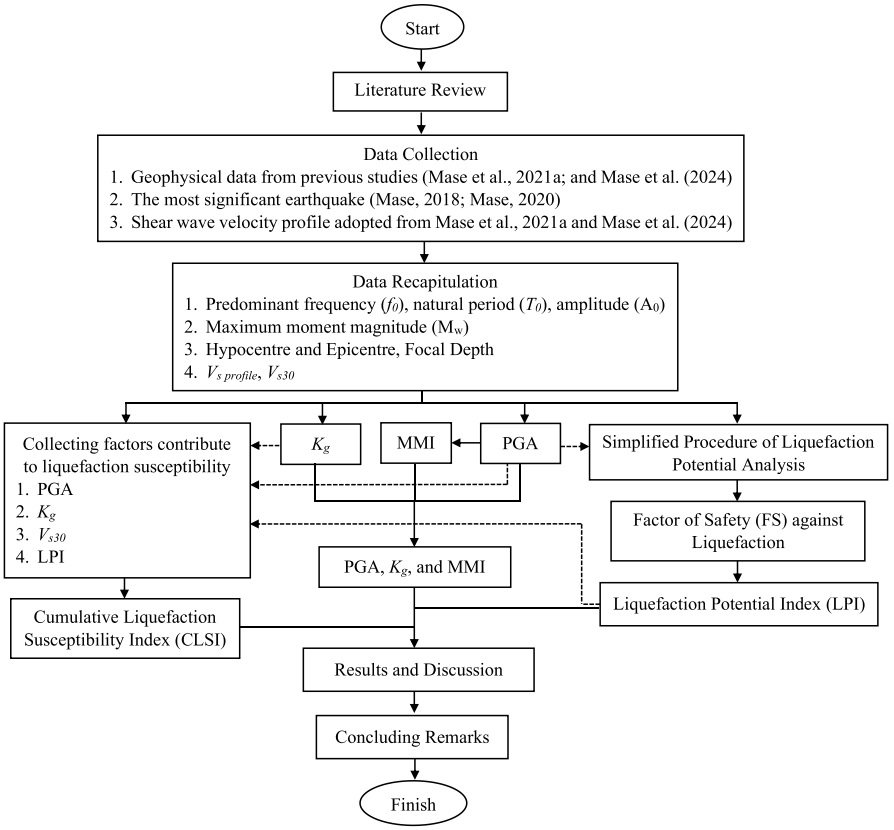

Fig. 4 Research framework

study area. Several parameters, such as PGA, LPI, K_g, and V_{s30}, are used to develop the index. The procedure of analysis is performed based on weighted analysis. The model is then expected to be used in engineering practice to predict liquefaction susceptibility. In general, the results of this study could contribute to supporting seismic hazard mitigation in Bengkulu City, which the local government can use to improve spatial planning considering the basis of seismic hazard.

4 Results and Discussions

4.1 Analyses Data

Table 1 presents the analysed data in this study. It should be noted that amplitude (A_0), predominant frequency (f_0), and natural period (T_0) are obtained based on ambient noise measurement under previous works, i.e. Mase et al. (2021a, 2024a). Table 1 also presents the hypocentre distance between the epicentre of the

Table 1 List of geophysical data (A_0, f_0, T_0) and hypocentre for each investigated site

No	Sites	Longitude (°)	Latitude (°)	Hypocentre (km)	A_0	f_0 (Hz)	T_0 (s)
1	Epicentre	101.502	− 4.407	–	–	–	–
2	SS-1	102.263	− 3.770	143.1422	2.563	5.206	0.192
3	SS-2	102.288	− 3.788	145.4900	1.194	2.834	0.353
4	SS-3	102.265	− 3.786	141.2595	3.077	6.717	0.149
5	SS-4	102.273	− 3.787	142.6525	1.343	0.75	1.333
6	SS-5	102.316	− 3.788	151.1635	1.59	1.47	0.680
7	SS-6	102.270	− 3.782	142.8432	8.561	0.6884	1.453
8	SS-7	102.299	− 3.789	147.5014	1.879	6.055	0.165
9	SS-8	102.323	− 3.789	152.4648	2.03	16.994	0.059
10	SS-9	102.263	− 3.777	142.2181	2.972	8.956	0.112
11	SS-10	102.266	− 3.785	141.5625	3.311	7.224	0.138
12	SS-11	102.279	− 3.785	144.1897	2.186	4.072	0.246
13	SS-12	102.295	− 3.784	147.5458	3.421	1.099	0.910
14	SS-13	102.325	− 3.795	152.0436	0.937	1.284	0.779
15	SS-14	102.304	− 3.790	148.4284	2.007	2.011	0.497
16	SS-15	102.309	− 3.788	149.7281	2.694	1.024	0.977
17	SS-16	102.320	− 3.786	152.3237	2.747	4.36	0.229
18	SS-17	102.312	− 3.792	149.7164	4.146	1.974	0.507
19	SS-18	102.317	− 3.794	150.5274	2.122	3.772	0.265
20	SS-19	102.299	− 3.793	146.9958	1.852	4.566	0.219
21	SS-20	102.290	− 3.785	146.3613	3.834	0.837	1.195
22	SS-21	102.285	− 3.785	145.3159	3.321	0.871	1.148
23	SS-22	102.295	− 3.789	146.7506	3.191	1.994	0.502
24	SS-23	102.300	− 3.785	148.3701	2.327	7.407	0.135
25	SS-24	102.331	− 3.781	155.2714	3.364	4.671	0.214
26	SS-25	102.331	− 3.790	153.9959	2.901	1.196	0.836
27	TS-1	102.248	− 3.789	137.5723	12.4637	15.564	0.064
28	TS-2	102.256	− 3.786	139.6407	10.746	13.7786	0.073
29	TS-3	102.249	− 3.786	138.2728	9.675	12.7891	0.078
30	TS-4	102.249	− 3.793	137.1926	8.786	12.7891	0.078
31	TS-5	102.253	− 3.793	138.0068	5.457	6.3005	0.159
32	TS-6	102.260	− 3.784	140.5978	4.8057	8.488	0.118
33	TS-7	102.250	− 3.789	137.8311	10.413	15.4082	0.065
34	TS-8	102.251	− 3.796	137.1698	5.12567	7.04567	0.142

Bengkulu-Mentawai Earthquake in 2007 and the investigated sites. From the data listed in Table 1, the histogram and frequency polygon are presented in Fig. 5. Based on statistical analysis of the data range for A_0, f_0, and T_0, the number of classes is seven. Figure 5a presents the distribution of A_0. It can be observed that A_0, with a range of 0.94 to 2.86, is dominant in the study area, whereas A_0, ranging from 6.70 to 8.62, is rarely found in the study area. Figure 5b presents for f_0 that, based on

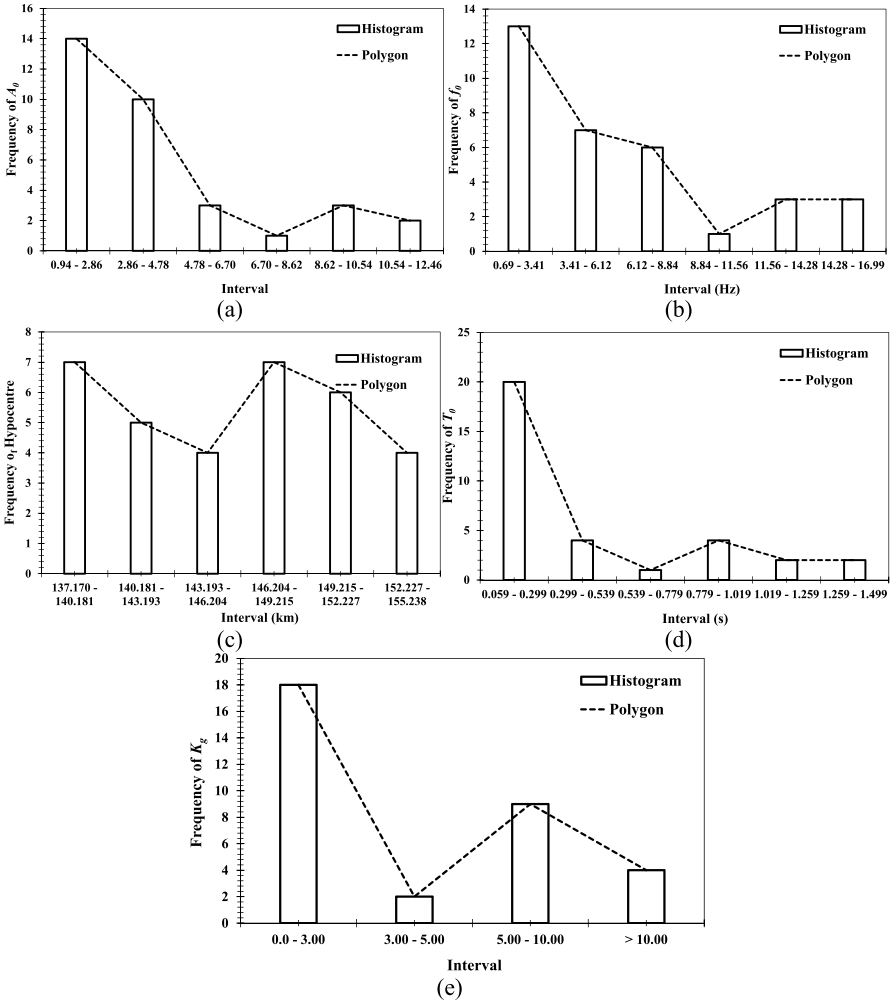

Fig. 5 Histogram and frequency polygon for **a** A_0, **b** f_0, **c** hypocentre, **d** T_0, **e** K_g

statistical analysis, is divided into six classes. f_0 ranging from 0.69 to 3.41 Hz are generally found in the study area, whereas f_0 ranging from 8.84 to 11.54 Hz is the least amount. Regarding T_0 (Fig. 5d), the period ranging from 0.059 to 0.299 s is the most in number, whereas 0.539 to 0.779 s is the least amount. Figure 5c presents the histogram and frequency polygon for hypocentre distance in which there are two central distance ranges, i.e. 137 to 140 km and 146 to 149 km, respectively. The hypocentre distance will be used to estimate peak ground acceleration on each investigated site, together with T_0.

Generally, a large A_0 indicates a significant contrast between bedrock and sediment, and a low f_0 indicates a soft sediment thickness (Gosar and Lenart 2010). Nakamura (2019) suggested that the combination between A_0 and f_0 can be used to

estimate the seismic vulnerability index or K_g. K_g can be the preliminary justification for the site's vulnerability to seismic impact (Akkaya 2020). Figure 5e presents the distribution of K_g based on classes divided by Akkaya (2020). It can be estimated that sites with low seismic vulnerability generally dominate the study area because K_g ranges from 0 to 3. However, several sites are also categorised as high seismic vulnerability. Since the study is generally dominated by low amplitude; therefore, K_g is also small. Farid and Mase (2020) suggested that based on the prediction of seismic vulnerability and ground shear strain during the Bengkulu-Enggano Earthquake 2000, K_g in Bengkulu City varied from low to very high seismic vulnerability. Specifically, seismic impacts such as crack settlement and liquefaction are present along the study area, especially near the coastline and estuary area. Mase et al. (2024a) also suggested a similar result to this study, in which, in the majority, the low seismic vulnerability zone is distributed in the eastern part to the middle part of Muara Bangkahulu downstream. A high to very high seismic vulnerability is generally found in areas in the western part.

4.2 Peak Ground Acceleration (PGA)

Figure 6 presents the distribution of PGA in the study area based on Kanai's model (Douglas 2021). In Fig. 6, PGA is divided into three classes, representing the motion's category based on the National Design Code of Indonesia of SNI 1726:2019 (SNI 1726: 2019 (2019)). The first category is weak motion, in which PGA is less than 0.17 g. PGA within 0.17 to 0.53 g is categorised as moderate motion, and PGA more than 0.53 g is defined as solid motion. Based on the results, it can be observed that PGA during the Bengkulu-Mentawai Earthquake in 2007 is categorised as moderate motion. However, areas in the western part indicate a strong motion (red

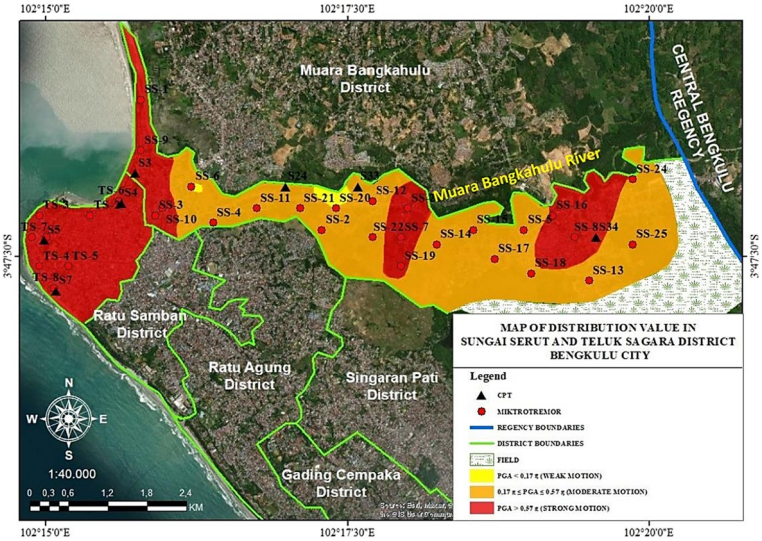

Fig. 6 Distribution of PGA

shading). A small zone of weak motion (yellow shading) was also found in the middle of the study area. It should be noted that PGA is controlled by earthquake energy and site characteristics (Yao et al. 2021). Areas in the eastern part tend to be far from the earthquake epicentre. In addition, based on Mase et al. (2024a) and Farid and Mase (2020), a high f_0 or a low T_0 is generally found in the western part of the study area. Gosar (Gosar 2010) mentioned a high f_0 reflects the soft sediment thickness or shallow bedrock. It is also consistent with Mase et al. (2024a) that the western part's bedrock is generally shallow. Parihar and Anbazhagan (2020) mentioned that the amplification generally occurred for a short period at thin sediment thickness. Since the study area sites (especially in the western part) are dominated by a short natural period, resonance could generally occur. Therefore, the PGA in this zone is relatively more significant than in other zones. In addition, the western part of the study area is where the local people are generally centralised as a socio-economic zone. Several infrastructures exist, such as offices, ports, local markets, and tourist-historical places. Those sectors are essential to support the city's development. In line with the findings of this study, the PGA map can be used as a reference to develop the western part of the area.

4.3 Modified Mercalli Intensity

From the distribution of PGA, the potential seismic damage in the MMI Scale is predicted, as shown in Fig. 7. Based on the figure, it can be observed that the potential seismic damage in the study area is generally IX in the MMI Scale. This is consistent with the prediction made by Mase et al. (2023b), who mentioned that Scale IX in MMI is dominant. Scale IX means "Damage is considerable in specially designed structures; well-designed frame structures are thrown off-kilter. Damage is

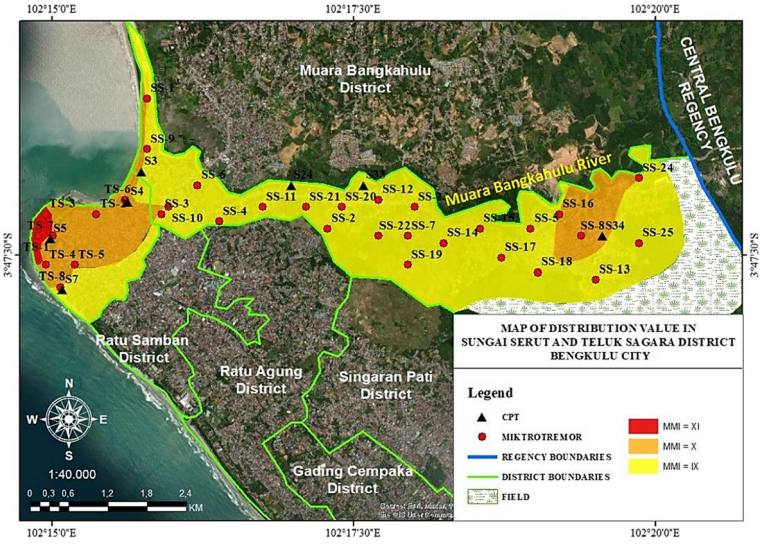

Fig. 7 Distribution of MMI

great in substantial buildings, with partial collapse. Buildings are shifted off foundations. Liquefaction occurs. Underground pipes are broken". Those damage types are also reported by site surveys, as reported by Hausler and Anderson (2007) and Mase et al. (2023b). Based on the prediction, liquefaction damage could occur in the study area. This is also generally consistent with fact-finding reported by Mase et al. (2023b). Scale IX (yellow shading) and Scale X (orange shading) are also predicted at sites in the eastern and western parts of the study areas. Scale XI (red shading) is generally found in the coastline of the study area, which is also found to have a high seismic vulnerability based on Mase et al. (2024a). Therefore, the prediction is generally consistent with previous studies. Implementing seismic hazard mitigation for the coastline area is vital to support the city's development. Government and private infrastructures were found in the coastline zone and generally collapsed during the earthquake in 2007. It indicates that the enforcement of structural performance during earthquakes should be improved. Regulations in the form of seismic design codes should be carefully considered when designing and constructing processes.

The damage intensity level is related to the earthquake characteristics and structural performance (Askan and Yucemen 2010). Ventura et al. (2005) mentioned that the enforcement of the implementation of seismic design code is critical to minimise potential seismic damage. It has been known that the MMI level is subjective because it is related to the quality of structures (Askan and Yucemen 2010). A structure based on the authorised seismic design code follows the seismic resistance design criteria. The seismic resistance design can be derived based on deterministic seismic hazard analysis or probabilistic seismic hazard analysis (Irsyam et al. 2015). In Indonesia, the enforcement of seismic design codes has been well-established within the last 20 years. The increase in seismic intensity in Indonesia, including Bengkulu City, pushes the structural building, especially for government assets, to follow the criteria. Therefore, MMI level mapping aims to observe the possibility of maximum damage in an area, which can be used to improve seismic hazard mitigation in the study area.

4.4 Factor of Safety (FS)

Using a semi-empirical approach, the liquefaction potential analysis is performed. To be consistent with the previous section, the representative sites presented in Fig. 2 are recalled to present the liquefaction potential in the study area. Figure 8 presents the study area's FS against liquefaction (FS) versus depth. Figure 8a (SS24) shows that the first three sand layers are predicted to undergo liquefaction. For site SS12 (Fig. 8b), the liquefied layers are not identified, whereas at site SS9 (Fig. 8c), all the analysed layers tend to undergo liquefaction. For TS7 (Fig. 8d), a site close to the coastal area tends to have three sand layers that are potentially liquefied. PGA distribution shows that PGA as the primary input of cyclic stress ratio indicates liquefaction because the values exceeded the threshold of liquefaction, i.e. 0.1 g (Kramer 1996). The combination of shallow groundwater levels, soil composting sites, and low soil resistance could increase liquefaction potential in the study area. According to Farid and Mase (2020), estimating ground shear strain based on

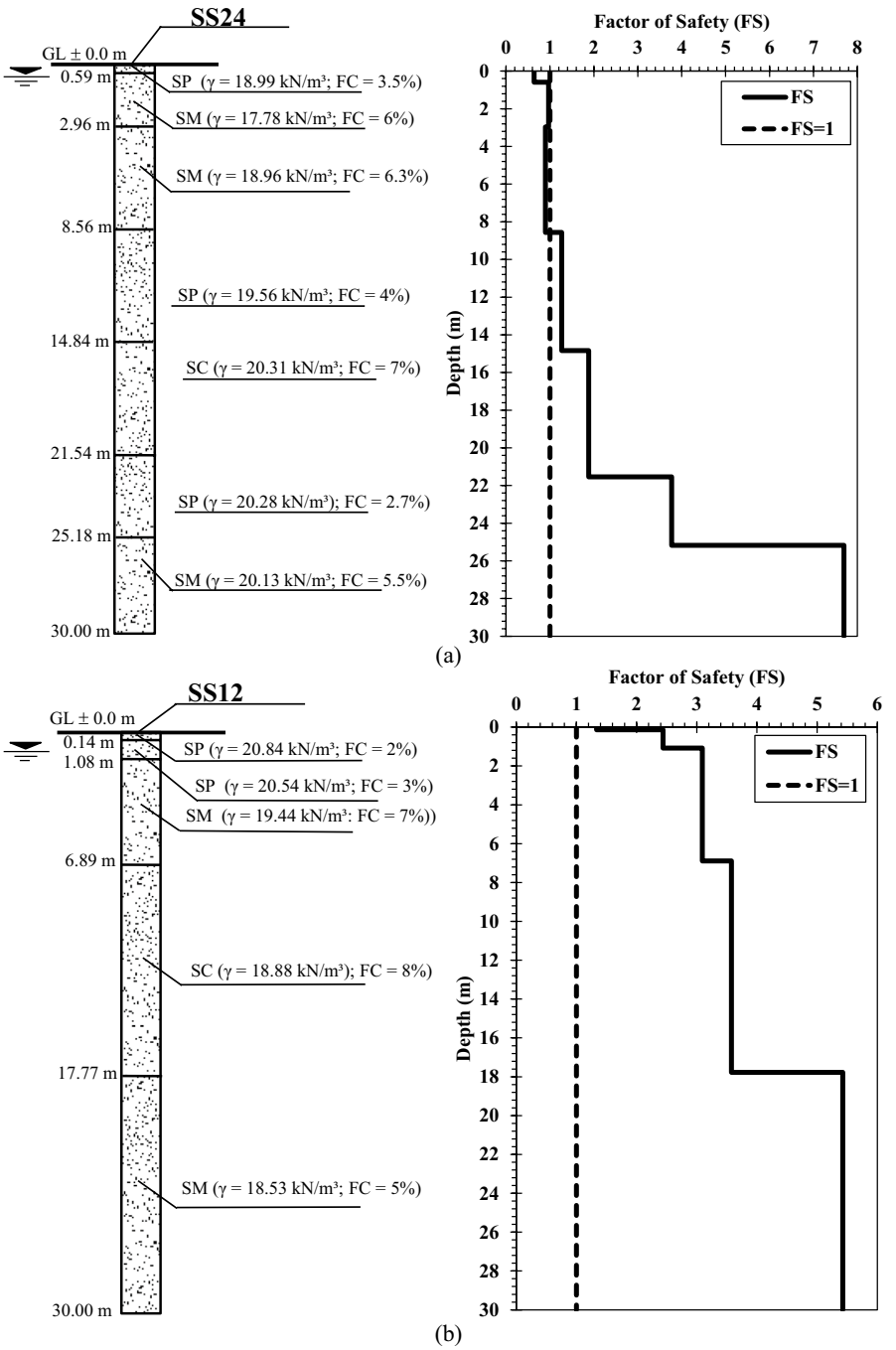

Fig. 8 FS against liquefaction vs depth for **a** SS24, **b** SS12, **c** SS9, and **d** TS7

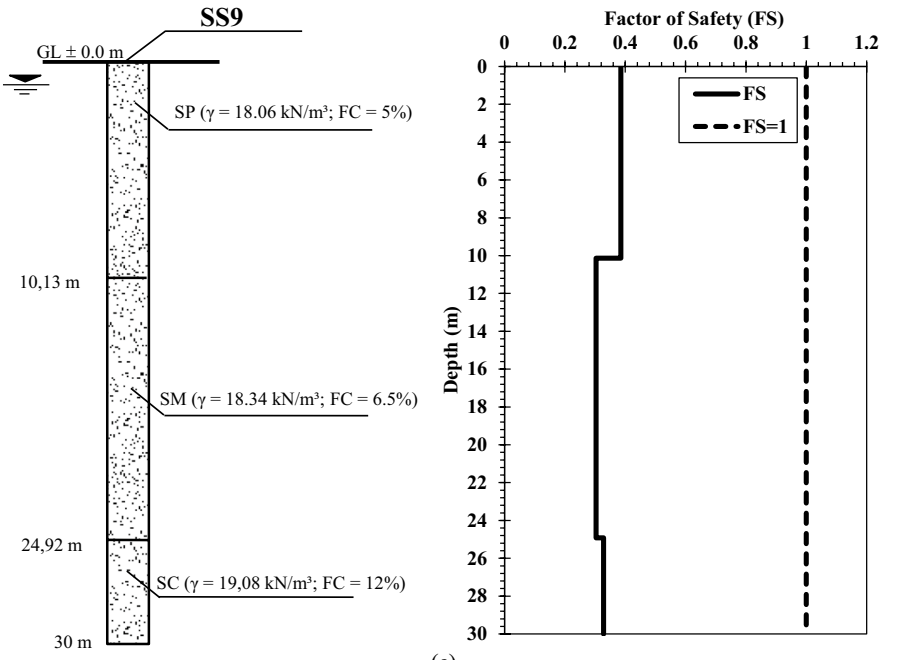

(c)

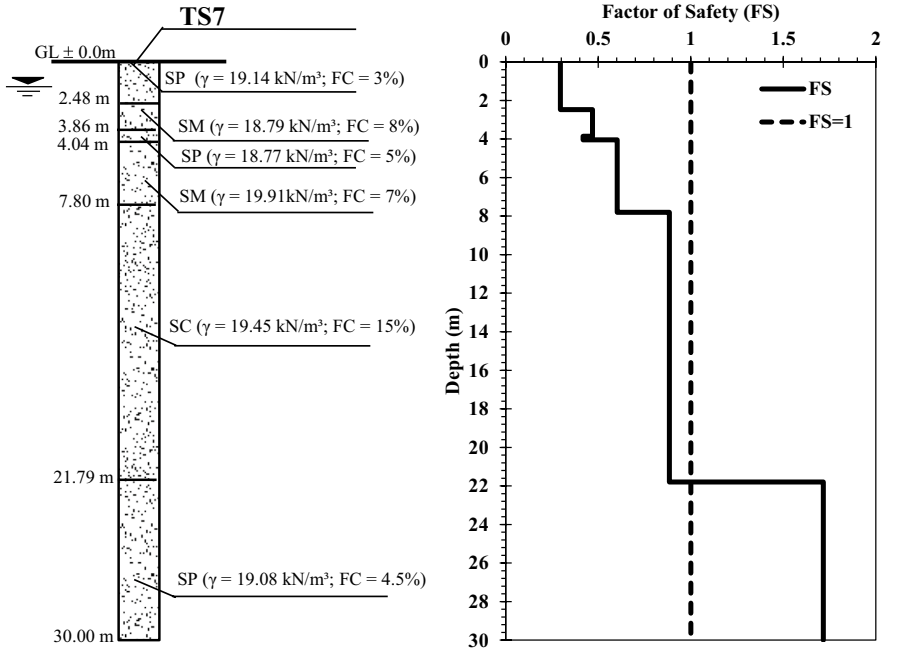

(d)

Fig. 8 (continued)

geophysical characteristics leads to the conclusion that liquefaction and crack settlement could happen in the study area, especially from the middle part of the coastline and estuary zone.

The representative sites reflect several activities in the study area; for example, SS24 is categorised as a high-terrain area where the time-averaged shear wave velocity for the first 30 m depth is significant and classified as Site Class D (Mase, et al. 2021a, 2024a). SS12 represents the market zone in the study area, which tends to have no liquefaction potential because of relatively low soil resistance and a low PGA during the earthquake. SS9, located at the local heritage zone in Bengkulu City, tends to have a severe liquefaction potential. This may be caused by low soil resistance and sandy soil under saturated conditions, which could be liquefied under a large PGA produced by the earthquake in 2007. Stewart and Knox (1995) suggested that liquefaction could also happen at a deeper depth. In general, sand layers classified as SM and SP are vulnerable to liquefaction in the study area. Liquefaction is determined based on the earthquake characteristics and soil conditions (Sukkarak et al. 2021; Liyanapathirana and Poulos 2004; Huang and Yu 2013). TS7, located at the centre of activity for coastline citizens, tends to have a severe liquefaction potential due to a site characteristic identified as a very high seismic vulnerability and a large PGA produced during the earthquake. Since the complexity of local characteristics along the river, it is important to improve seismic hazard mitigation in the study area.

4.5 Liquefaction Potential Index (LPI)

FS corresponding to depth is implemented to determine LPI in the study area. Using the numerical integration concept, the LPI for the study area can be generated. In line with the representative sites, Figs. 9a–d represents SS24, SS12, SS9, and TS7, respectively. For SS24 (Fig. 9a), LPI is 7.6, which indicates marginal liquefaction, whereas for SS12 (Fig. 9b), LPI is zero, which indicates no liquefaction. LPI of 47.12 is indicated at Siet SS9 (Fig. 9c), indicating severe liquefaction. For the last representative site, TS-7, the LPI value is 25.11, indicating severe liquefaction.

Figure 10 presents the hazard map of liquefaction based on LPI. In general, there are two main categories of liquefaction potential in the study area. A severe liquefaction potential is generally found in the estuary, coastal areas, and the study area's southern and middle parts. A moderate liquefaction potential is also found in the eastern part to the middle part of the study area. Several areas in the upper zone of the study area are categorised as having no liquefaction potential, and some thin zones in the middle zone of the study area have marginal liquefaction potential.

Figure 10 also explains that coastal areas and estuary zones tend to have a severe liquefaction potential. This zone is now the mainstay area supporting the socio-economics aspect along the river. Several tourist zones and traditional restaurants are generally found. In line with this condition, Gomez-Martinez (2020) suggested that the enforcement of foundation design considering the potential impact of liquefaction should be addressed. Brevik and Miller (2015) and Vessia et al. (2021) explained that a detailed geological study should improve soil resistance for areas

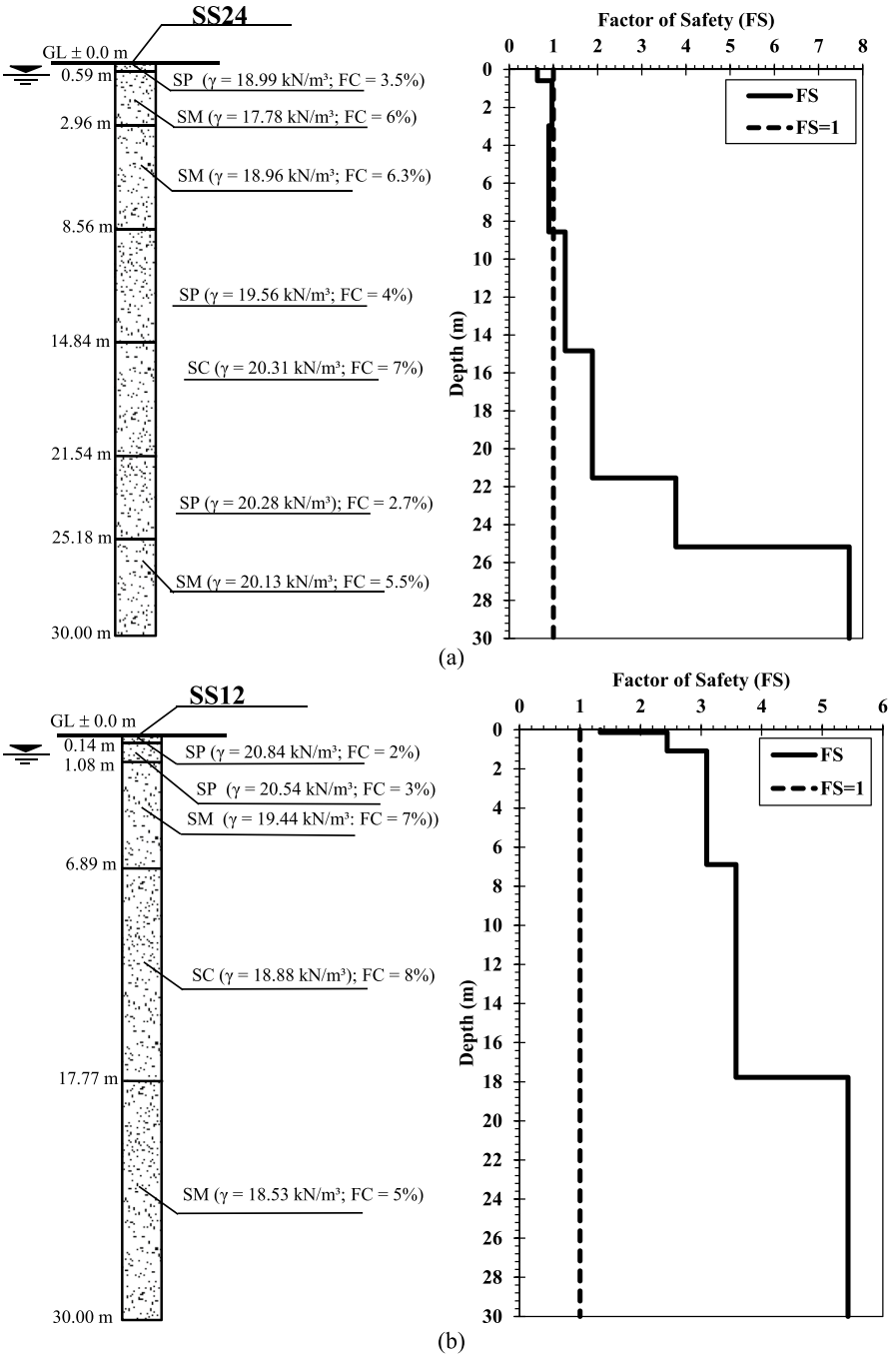

Fig. 9 LPI for **a** SS24, **b** SS12, **c** SS9, **d** TS7

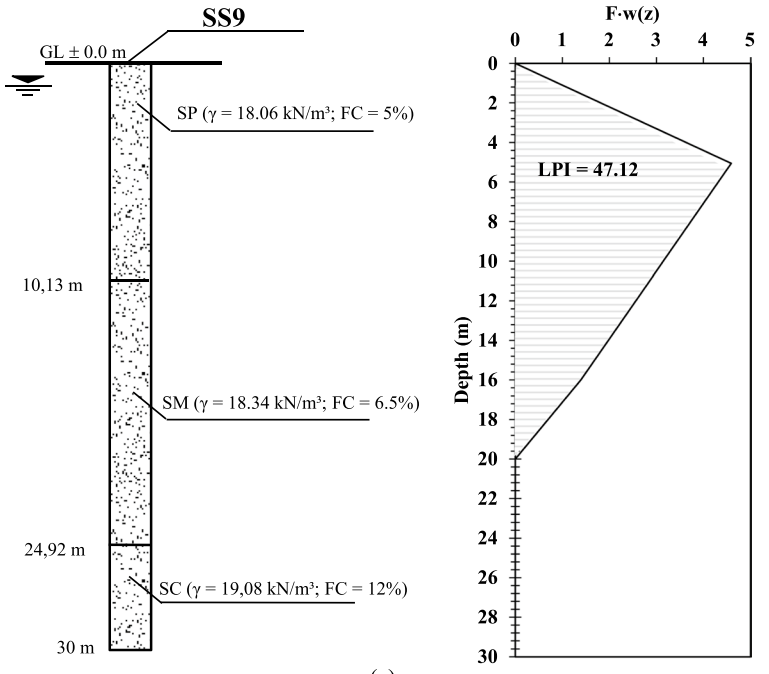

(c)

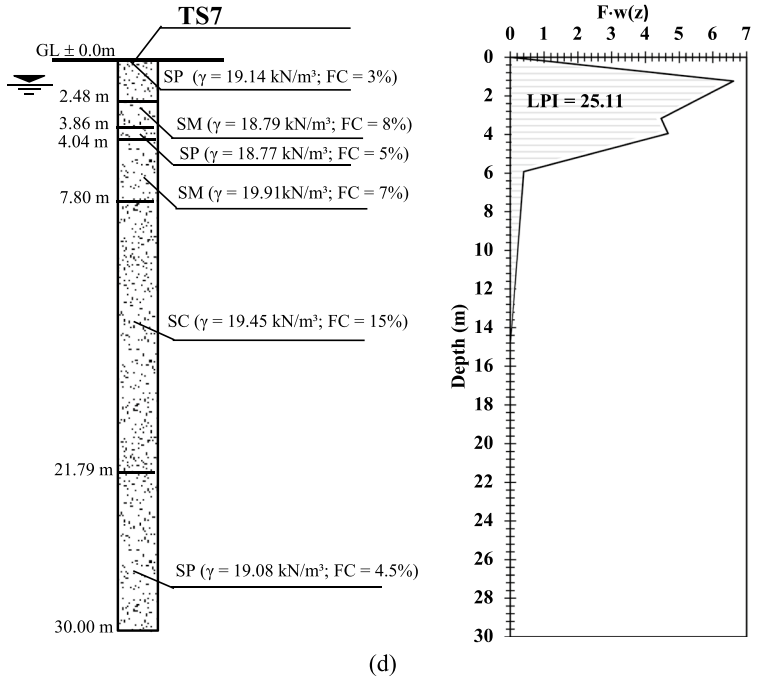

(d)

Fig. 9 (continued)

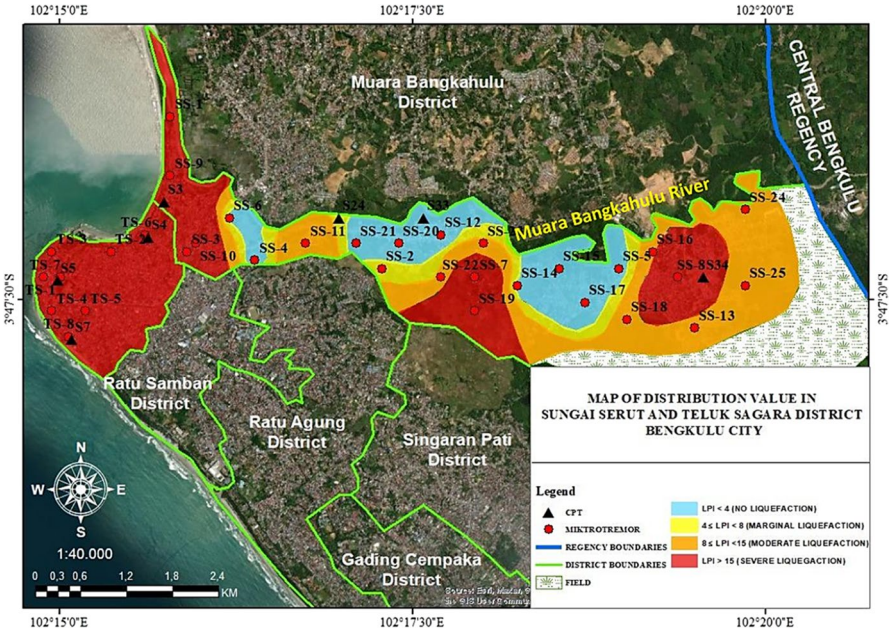

Fig. 10 The map of LPI

with high seismic impact potential. The concern should also be addressed for areas with a moderate liquefaction potential, especially if a stronger earthquake event could happen (Karpouza et al. 2021; Abbas et al. 2021; Allstadt et al. 2022; Ko et al. 2023). Areas with moderate zones are generally located in the flood plain, which is also vulnerable to seismic impact. In addition, areas under this kind of liquefaction potential tend to be housing zones, where people are generally centralised. Spatial development based on seismic hazards should be addressed to minimise liquefaction potential during earthquakes.

4.6 Liquefaction Susceptibility and Further Development of Method

As elaborated in the previous section, liquefaction susceptibility should be viewed from all aspects. Regarding susceptibility, several liquefaction hazard parameters could be considered the most contributing factors. Table 2 lists the liquefaction hazard parameters to construct CLSI. Table 3 presents the statistical parameters for considered liquefaction susceptibility factors. Table 3 shows that minimum, maximum, and average values and standard deviation for PGA are 0.191 g, 0.962 g, 0.497 g, and 0.249, respectively. V_{s30} is obtained from a previous study by Mase et al. (2021a). The statistical parameters for V_{s30} are 251, 451, 333, and 55 m/s. Statistical parameters for K_g are 0.242, 106.465, 7.470, and 18, respectively, whereas for LPI, they are 0, 50.168, 16.741, and 16, respectively.

Table 2 List of liquefaction susceptibility considered factors

	Longitude (°)	Latitude (°)	V_{s30} (m/s)	K_g	PGA (g)	LPI
SS-1	102.263	− 3.770	294	1.262	0.524	35.527
SS-2	102.288	− 3.788	271	0.503	0.377	6.529
SS-3	102.265	− 3.786	321	1.410	0.607	41.313
SS-4	102.273	− 3.787	279	2.405	0.200	0.000
SS-5	102.316	− 3.788	385	1.720	0.256	0.000
SS-6	102.270	− 3.782	251	106.465	0.191	0.000
SS-7	102.299	− 3.789	264	0.583	0.539	36.236
SS-8	102.323	− 3.789	388	0.242	0.859	50.168
SS-9	102.263	− 3.777	287	0.986	0.694	47.118
SS-10	102.266	− 3.785	298	1.518	0.627	41.576
SS-11	102.279	− 3.785	277	1.174	0.458	19.803
SS-12	102.295	− 3.784	300	10.649	0.230	0.000
SS-13	102.325	− 3.795	339	0.684	0.237	1.474
SS-14	102.304	− 3.790	389	2.003	0.308	0.000
SS-15	102.309	− 3.788	377	7.088	0.217	0.000
SS-16	102.320	− 3.786	441	1.731	0.436	13.820
SS-17	102.312	− 3.792	451	8.708	0.301	0.000
SS-18	102.317	− 3.794	438	1.194	0.413	11.591
SS-19	102.299	− 3.793	273	0.751	0.471	31.114
SS-20	102.290	− 3.785	260	17.562	0.203	0.000
SS-21	102.285	− 3.785	270	12.663	0.209	0.000
SS-22	102.295	− 3.789	279	5.107	0.312	8.370
SS-23	102.300	− 3.785	303	0.731	0.591	9.492
SS-24	102.331	− 3.781	362	2.423	0.438	6.836
SS-25	102.331	− 3.790	362	7.037	0.224	0.000
TS-1	102.248	− 3.789	360	9.981	0.962	15.089
TS-2	102.256	− 3.786	357	8.381	0.885	23.843
TS-3	102.249	− 3.786	374	7.319	0.865	27.148
TS-4	102.249	− 3.793	358	6.036	0.876	16.644
TS-5	102.253	− 3.793	350	4.726	0.609	16.943
TS-6	102.260	− 3.784	356	2.721	0.687	28.100
TS-7	102.250	− 3.789	332	7.037	0.954	25.107
TS-8	102.251	− 3.796	350	3.729	0.650	38.598

Table 3 Statistical parameters

Parameters	PGA (g)	V_{s30} (m/s)	K_g	LPI	CLSI
Minimum value	0.191	251	0.242	0.000	7
Maximum value	0.962	451	106.465	50.168	14
Average value	0.497	333	7.470	16.741	11
Standard deviation	0.249	55	18	16	2

From the information listed in Table 2, the CLSI map is generated based on weighted method analysis, as presented in Fig. 11. From the figure, it can be observed that the study area generally has a moderate liquefaction susceptibility. The high liquefaction susceptibility in the study area is generally located in the western part of the study area or the coastal area. This is reasonable because the K_g value is generally high, the PGA value is high, the LPI is high, and V_{s30} is generally low. Those parameters played an essential role in controlling the massive impact of the earthquake in 2007. Fact findings reported by Hausler and Anderson (2007), Farid and Mase (2020), and Mase et al. (2023b) generally fall to the point that coastal areas are susceptible to undergoing liquefaction. A small zone with low liquefaction susceptibility is also found in the central part of the study area. The implemented CLSI procedure could provide an objective perspective of liquefaction potential in the study area. For dominant areas, moderate liquefaction susceptibility during the earthquake in 2007, the indication of liquefaction was not identified because the impact was insignificant compared to the red zone area (coastal area). Therefore, the implementation of CLSI is also reasonable for this case study.

As a parameter that reflects liquefaction susceptibility, LPI could play an essential role in determining CLSI. In its development, LPI has significantly improved. Maurer et al. (2014) and Maurer et al. (2015) suggested that recent cases should update the zoning criteria of LPI, and the LPI calculation procedure should also consider the unliquefiable surface layer, especially for areas not dominated by sand. For areas having sandy, the original LPI method is still applicable, but for areas having various soil types, the LPI calculation, as suggested by Maurer et al. (2015), should be

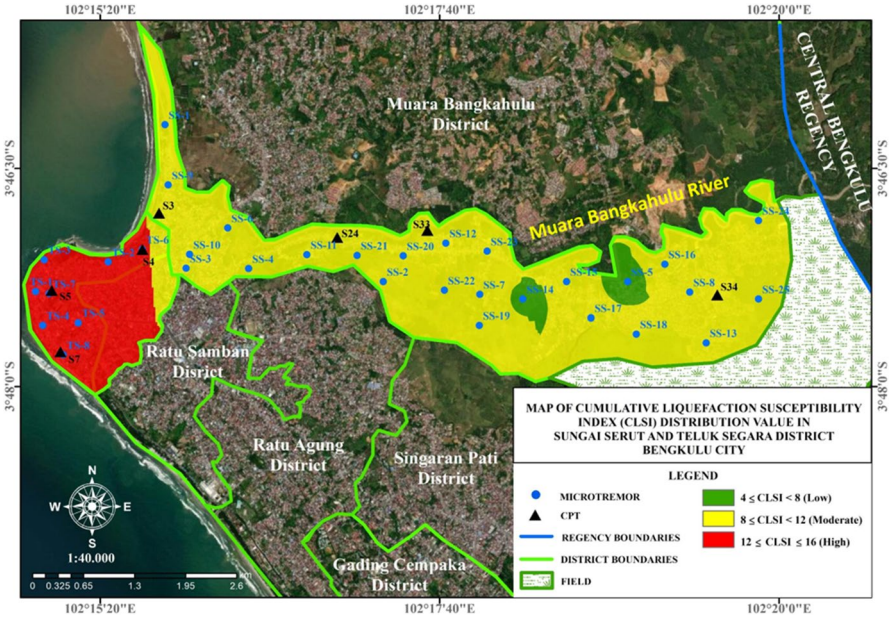

Fig. 11 The map of CLSI

adopted. Therefore, in the CLSI method, the development of knowledge on liquefaction prediction could dynamically change the estimation of LPI. The CLSI method integrates all mindsets, which can contribute to determining the liquefaction.

Besides quantifying liquefaction potential, the considered earthquake in the analysis is not only related to the deterministic approach. Another hazard assessment approach, such as probabilistic seismic hazard analysis, could also be adapted to determine (LPI) and PGA, as suggested by Makdisi and Kramer (2024). Those parameters are also components of the CLSI method. In line with seismic hazard assessment, CLSI is also applicable to accommodate the hazard approach for liquefaction susceptibility mapping.

This aligns with the overview of the CLSI method as the integrated approach to estimating liquefaction potential. It should also be noted that the implementation of CLSI should be performed for sites having liquefaction potential; in other words, the application of this method is limited to sandy soil sites only. The advantage of the CLSI method is that it could reflect the integrated liquefaction susceptibility in one frame that is generally consistent with the field evidence for a case study of Bengkulu City. Furthermore, the CLSI method could be implemented in other areas to depict the liquefaction susceptibility in other areas. In general, the distribution of liquefaction susceptibility is essential for further countermeasure action. Several methods, such as geotextile infiltration (Indhanu et al. 2023), partial saturation (Seyedi-Viand and Eseller-Bayat 2022), drainage (Farzalizadeh et al. 2021), and wasting material (Hazarika et al. 2020), could be alternatives to mitigate liquefaction. Swasdi et al. (2024) also suggested that selecting the structure's foundation is important to accommodate the acting forces. In addition, the development of liquefaction potential analysis using artificial neuron network (ANN), the method of liquefaction potential analysis is now more developed. The parameters influencing liquefaction, such as PGA, water content, fines content, and soil resistance, are generally trained to predict factors of safety against liquefaction (Ghani and Kumari 2022). Those parameters are also analysed based on a random search, grid search, and Bayesian optimisation (Kurnaz et al. 2023). In line with the advanced liquefaction potential analysis, the CLSI method could be combined with artificial intelligence to seek liquefaction susceptibility. The connection between the CLSI method and liquefaction countermeasure and liquefaction susceptibility and the enhancement of the CLSI method in ANN will be presented in further study to accommodate the importance of liquefaction countermeasure.

5 Conclusions

This paper presents the cumulative liquefaction susceptibility index (CLSI) to predict liquefaction impact (a case study of Muara Bangkahulu's downstream areas, Bengkulu City, Indonesia). The liquefaction potential analysis is performed based on ground motion prediction and site condition. The hazard zonation during an earthquake is discussed. A new method called CLSI was developed in this study to provide a better understanding of liquefaction susceptibility. Several concluding remarks can be drawn in the following points:

1. Site characteristics are essential in determining liquefaction severity. Combining site characteristics and earthquake impacts could lead to an area's liquefaction potential. PGA and damage intensity levels are generally consistent with previous studies. As found in coastal areas, PGA at shallow bedrock is relatively large. PGA and K_g are generally consistent in predicting the potential seismic damage, especially for areas on the coastline. The damage intensity level is also generally consistent with previous studies. The enforcement of a national seismic design code should be implemented to reduce the potential seismic damage.
2. LPI is a parameter that depicts liquefaction potential and could be a basis for preliminary investigation to study liquefaction susceptibility. However, LPI should be supported by several sites, geophysical, and earthquake parameters to provide an integrated liquefaction susceptibility perspective. In addition, the zoning criteria of liquefaction based on recent cases and geological conditions considering liquefiable and unliquefiable layers should also be considered in LPI analysis. Therefore, in the CLSI method, the LPI analysis could be dynamically adapted with confirmed cases, and it should be consistent with the criteria of liquefaction zones used in CLSI. Other aspects, such as seismic hazard assessment, could also determine CLSI results. Both deterministic and probabilistic approaches can be used to estimate LPI and PGA values for CLSI.
3. A method of CLSI could be the solution to explain general information about liquefaction susceptibility. Factors contributing to controlling liquefaction potential are included in conducting CLSI analysis. This means that the results from the CLSI method are more integrated than those of other methods, which separately interpret liquefaction hazards based on safety and probability. The spatial development can consider the CLSI method to provide a better description of seismic hazard mitigation. The CLSI method implemented in this study provides a better description that is generally consistent with previous studies. The method's implementation could be enhanced in other areas in the future.
4. This study proposes an integrated approach to liquefaction susceptibility. However, the procedure to quantify liquefaction hazard based on an integrated approach, including vulnerability, susceptibility, risk, and capacity, is still limited. It will be presented in further studies.
5. This study still focuses on developing a new mapping method for liquefaction susceptibility. However, the recommendation for liquefaction countermeasures linked to the distribution of liquefaction susceptibility is still limited. Therefore, a study connecting the liquefaction susceptibility with the liquefaction countermeasure recommendation can be conducted in the future.

Acknowledgements This study was supported by the research fund from the University of Bengkulu under the competitive research scheme with grant no. 2183/UN30.15/LT/2019. The work was also performed in collaboration with the Japan-ASEAN Science and Technology Innovation Platform (JASTIP-WP4) 2024.

Author's contributions Lindung Zalbuin Mase: conceptualization, methodology, data analysis visualization, writing—review and editing, project administration.

Funding It is not applicable in this case.

Data Availability All the datasets used and analysed during the current study are available from the corresponding author at reasonable request.

Declarations

Ethics Approval and Consent to Participate Not applicable.

Consent for Publication The author has read and agreed to the published version of the manuscript.

Competing Interests The author declares no competing interests.

References

Abbas, M., Elbaz, K., Shen, S.L., et al.: Earthquake effects on civil engineering structures and perspective mitigation solutions: a review. Arab. J. Geosci. **14**, 1350 (2021). https://doi.org/10.1007/s12517-021-07664-5

Akkaya, İ: Availability of seismic vulnerability index (Kg) in the assessment of building damage in Van, Eastern Turkey. Earthq. Eng. Eng. Vib. **19**(1), 189–204 (2020). https://doi.org/10.1007/s11803-020-0556-z

Allstadt, K.E., Thompson, E.M., Jibson, R.W., Wald, D.J., Hearne, M., Hunter, E.J., Haynie, K.L.: The US Geological Survey ground failure product: Near-real-time estimates of earthquake-triggered landslides and liquefaction. Earthquake Spectra **38**(1), 5–36 (2022). https://doi.org/10.1177/8755293021103268 5

Ambikapathy, A., Catherine, J.K., Gahalaut, V.K., et al.: The 2007 Bengkulu earthquake, its rupture model and implications for seismic hazard. J. Earth Syst. Sci. **119**, 553–560 (2010). https://doi.org/10.1007/s12040-010-0037-2

Andrus, R.D., Stokoe, K.H., II.: Liquefaction resistance of soils from shear-wave velocity. Journal of Geotechnical and Geoenvironmental Engineering **126**(11), 1015–1025 (2000). https://doi.org/10.1061/(ASCE)1090-0241(2000)126:11(1015)

Andrus, R.D., Stokoe, K.H., Hsein Juang, C.: Guide for shear-wave-based liquefaction potential evaluation. Earthq. Spectra **20**(2), 285–308 (2004). https://doi.org/10.1193/1.1715106

Ansari, A., Zahoor, F., Rao, K.S., Jain, A.K.: Liquefaction hazard assessment in a seismically active region of Himalayas using geotechnical and geophysical investigations: a case study of the Jammu Region. Bull. Eng. Geol. Env. **81**(9), 349 (2022). https://doi.org/10.1007/s10064-022-02852-3

Askan, A., Yucemen, M.S.: Probabilistic methods for the estimation of potential seismic damage: Application to reinforced concrete buildings in Turkey. Struct. Saf. **32**(4), 262–271 (2010). https://doi.org/10.1016/j.strusafe.2010.04.001

Aytaş, Z., Alpaslan, N., Özçep, F.: Evaluation of liquefaction potential by standard penetration test and shear wave velocity methods: a case study. Nat. Hazards **118**(3), 2377–2417 (2023). https://doi.org/10.1007/s11069-023-06093-9

Ballegooy, S.V., Malan, P.J., Jacka, M.E., Lacrosse, V.I.M.F., Leeves, J.R., Lyth, J.E., Cowan, H.: Methods for characterising effects of liquefaction in terms of damage severity. In: Proceedings of the 15th world conference of earthquake engineering, Lisbon, Portugal 24–28, pp. 1–10. (2012).

Boulanger, R.W., Idriss, I.M.: CPT and SPT based liquefaction triggering procedures. In: Report No. UCD/CGM.-14, 1, 134. Department of Civil and Environmental Engineering, College of Engineering, University of California at Davis, USA, (2014)

Brevik, E.C., Miller, B.A.: The use of soil surveys to aid in geologic mapping with an emphasis on the Eastern and Midwestern United States. Soil Horizons **56**(4), 1–9 (2015). https://doi.org/10.2136/sh15-01-0001

Building Seismic Safety Council (BSSC): NEHRP (National Earthquake Hazards Reduction Program) Recommended Seismic Provisions for New Buildings and Other Structures (FEMA P-2082–1). In: Volume I: Part 1 Provisions and Part 2 Commentary, 2020th edn. Building Seismic Safety Council: a council of the National Institute of Building Sciences, Washington, D.C (2020)

Douglas, J.: Ground motion prediction equations 1964–2021. University of Strathclyde, UK, Department of Civil & Environmental Engineering (2021)

Farid, M., Mase, L.Z.: Implement seismic hazard mitigation based on ground shear strain indicator for a spatial plan of Bengkulu City. Indonesia. GEOMATE Journal **18**(69), 199–207 (2020). https://doi.org/10.21660/2020.69.24759

Farzalizadeh, R., Hasheminezhad, A., Bahadori, H.: Shaking table tests on wall-type gravel and rubber drains as a liquefaction countermeasure in silty sand. Geotext. Geomembr. **49**(6), 1483–1494 (2021). https://doi.org/10.1016/j.geotexmem.2021.06.002

Ghani, S., Kumari, S.: Liquefaction hazard mitigation using computational model considering sustainable development. In: Roshni, T., Samui, P., Bui, D.T., Kim, F., Khatibi, R. (eds.) Risk, reliability and sustainable remediation in the field of civil and environmental engineering, pp. 183–196. (2022). https://doi.org/10.1016/B978-0-323-85698-0.00023-X

Gomez-Martinez, F., Millen, M.D., Costa, P.A., Romao, X.: Estimation of the potential relevance of differential settlements in earthquake-induced liquefaction damage assessment. Eng. Struct. **211**, 110232 (2020). https://doi.org/10.1016/j.engstruct.2020.110232

Gosar, A.: Site effects and soil-structure resonance study in the Kobarid basin (NW Slovenia) using microtremors. Nat. Hazard. **10**(4), 761–772 (2010). https://doi.org/10.5194/nhess-10-761-2010

Gosar, A., Lenart, A.: Mapping the thickness of sediments in the Ljubljana Moor basin (Slovenia) using microtremors. Bull. Earthq. Eng. **8**(3), 501–518 (2010). https://doi.org/10.1007/s10518-009-9115-8

Hausler, E., Anderson, A.: Observation of the 12 and 13 September 2007 Earthquake, Sumatra, Indonesia. Build Change Report, Colorado, 15pp. (2007). https://buildchange-web.s3.amazonaws.com/resources/tech/BC_Bengkulu_English.pdf. Accessed 24 Jan 2024

Hazarika, H., Pasha, S.M.K., Ishibashi, I., Yoshimoto, N., Kinoshita, T., Endo, S., Hitosugi, T.: Tire-chip reinforced foundation as liquefaction countermeasure for residential buildings. Soils and Foundations **60**(2), 315–326 (2020). https://doi.org/10.1016/j.sandf.2019.12.013

Hollender, F., Cornou, C., Dechamp, A., Oghalaei, K., Renalier, F., Maufroy, E., Sicilia, D.: Characterization of site conditions (soil class, V_{S30}, velocity profiles) for 33 stations from the French permanent accelerometric network (RAP) using surface-wave methods. Bulletin of Earthquake Engineering **6**(6), 2337–2365 (2018). https://doi.org/10.1007/s10518-017-0135-5

Huang, Y., Yu, M.: Review of soil liquefaction characteristics during major earthquakes of the twenty-first century. Nat. Hazards **65**, 2375–2384 (2013). https://doi.org/10.1007/s11069-012-0433-9

Idriss, I.M., Boulanger, R.W.: Semi-empirical procedures for evaluating liquefaction potential during earthquakes. Soil Dyn. Earthq. Eng. **26**(2–4), 115–130 (2006). https://doi.org/10.1016/j.soildyn.2004.11.023

Indhanu, T., Srisakul, W., Chompoorat, T., et al.: Evaluation and mitigation of ground loss and shear failure in silty sand due to static liquefaction potential with geotextile filtration. Int. J. of Geosynth. and Ground Eng **9**, 80 (2023). https://doi.org/10.1007/s40891-023-00496-1

Irsyam, M., Hutabarat, D., Asrurifak, M., Imran, I., Widiyantoro, S., Hendriyawan, D., Sadisun, I., Hutapea, B., Afriansyah, T., Pindratno, H., Firmanti, A., Ridwan, M., Haridjono, S.W., Pandhu, R.: Development of seismic risk microzonation maps of Jakarta city. In: Iai, S. (ed.) Geotechnics for catastrophic flooding events, pp. 35–47. (2015). https://doi.org/10.1201/b17438-6

Iwasaki, T., Arakawa, T., Tokida, K.I.: Simplified procedures for assessing soil liquefaction during earthquakes. International Journal of Soil Dynamics and Earthquake Engineering **3**(1), 49–58 (1984). https://doi.org/10.1016/0261-7277(84)90027-5

Karpouza, M., Chousianitis, K., Bathrellos, G.D., et al.: Hazard zonation mapping of earthquake-induced secondary effects using spatial multi-criteria analysis. Nat. Hazards **109**, 637–669 (2021). https://doi.org/10.1007/s11069-021-04852-0

Kim, H.S., Kim, M., Baise, L.G., Kim, B.: Local and regional evaluation of liquefaction potential index and liquefaction severity number for liquefaction-induced sand boils in Pohang, South Korea. Soil Dyn. Earthq. Eng. **141**, 106459 (2021). https://doi.org/10.1016/j.soildyn.2020.106459

Ko, Y.Y., Tsai, C.C., Hwang, J.H., Hwang, Y.W., Ge, L., Chu, M.C.: Failure of engineering structures and associated geotechnical problems during the 2022 ML 6.8 Chihshang earthquake Taiwan. Nat. Hazards **118**(1), 55–94 (2023)

Kramer, S.L.: Geotechnical earthquake engineering. Chennai, India, Pearson Education (1996)

Kurnaz, T.F., Erden, C., Kökçam, A.H., Dağdeviren, U., Demir, A.S.: A hyper parameterized artificial neural network approach for prediction of the factor of safety against liquefaction. Eng. Geol. **319**, 107109 (2023). https://doi.org/10.1016/j.enggeo.2023.107109

Liyanapathirana, D.S., Poulos, H.G.: Assessment of soil liquefaction incorporating earthquake characteristics. Soil Dyn. Earthq. Eng. **24**(11), 867–875 (2004). https://doi.org/10.1016/j.soildyn.2003.11.010

Makdisi, A.J., Kramer, S.L.: Improved computational methods for probabilistic liquefaction hazard analysis. Soil Dyn. Earthq. Eng. **176**, 108272 (2024). https://doi.org/10.1016/j.soildyn.2023.108272

Mase, L.Z.: Shaking Table Test of Soil Liquefaction in Southern Yogyakarta. Int. J. Technol. **8**(4), 747–760 (2017). https://doi.org/10.14716/ijtech.v8i4.9488

Mase, L.Z.: Slope stability and erosion-sedimentation analyses along sub-watershed of Muara Bangkahulu River in Bengkulu City, Indonesia. In E3S Web of Conf. **148**, 03002 (2020). https://doi.org/10.1051/e3sconf/202014803002. (**EDP Sciences**)

Mase, L.Z.: Seismic hazard vulnerability of Bengkulu City, Indonesia, based on deterministic seismic hazard analysis. Geotech. Geol. Eng. **38**(5), 5433–5455 (2020). https://doi.org/10.1007/s10706-020-01375-6

Mase, L.Z., Refrizon, R., Anggraini, P.W.: Local site investigation and ground response analysis on downstream area of Muara Bangkahulu River, Bengkulu City, Indonesia. Indian Geotech J, vol. 51, pp. 952–966. (2021a). https://doi.org/10.1007/s40098-020-00480-w

Mase, L.Z.: Local seismic hazard map based on the response spectra of stiff and very dense soils in Bengkulu city Indonesia. Geodesy Geody. **13**(6), 573–584 (2022). https://doi.org/10.1016/j.geog.2022.05.003

Mase, L.Z., Amri, K., Farid, M., Rahmat, F., Fikri, M.N., Saputra, J., Likitlersuang, S.: Effect of water level fluctuation on riverbank stability at the estuary area of Muaro Kualo Segment, Muara Bangkahulu River in Bengkulu Indonesia. Eng. J. **26**(3), 1–16 (2022). https://doi.org/10.4186/ej.2022.26.3.1

Mase, L.Z., Sunanda, R., Utami, F., Wahyuni, M.S., Syafrizal, M.D., Putri, M.A., Keawsawasvong, S.: Slope Stability of Riverbank during Flood in Bengkulu City, Indonesia (A case study of Nakau Segment). In: Sci Technol Asia, pp. 125–142. (2023a) . https://ph02.tci-thaijo.org/index.php/SciTechAsia/article/view/249868

Mase, L.Z., Agustina, S., Hardiansyah, F.M., Supriani, F., Tanapalungkorn, W., Likitlersuang, S.: Application of simplified energy concept for liquefaction prediction in Bengkulu City Indonesia. Geotech. Geol. Eng. **41**(3), 1999–2021 (2023b). https://doi.org/10.1007/s10706-023-02388-7

Mase, L.Z., Irsyam, M., Gustiparani, D., Noptapia, A.N., Syahbana, A.J., Soebowo, E.: Identification of bedrock depth along a downstream segment of Muara Bangkahulu River, Bengkulu City. Indonesia. Bull. Eng. Geol. Env. **83**(4), 93 (2024a). https://doi.org/10.1007/s10064-024-03591-3

Mase, L.Z., Wahyuni, M.S., Hardiansyah, Syahbana, A.J.: Prediction of damage intensity level distribution in Bengkulu City, during the M_w 8.6 Bengkulu-Mentawai Earthquake in 2007, Indonesia. In: Transp. Infrastruct. Geotech, vol. 11, pp. 769–793. (2024b). https://doi.org/10.1007/s40515-023-00306-1

Maurer, B.W., Green, R.A., Cubrinovski, M., Bradley, B.A.: Evaluation of the liquefaction potential index for assessing liquefaction hazard in Christchurch, New Zealand. Journal of Geotechnical and Geoenvironmental Engineering **140**(7), 04014032 (2014). https://doi.org/10.1061/(ASCE)GT.1943-5606.0001117

Maurer, B.W., Green, R.A., Taylor, O.D.S.: Moving towards an improved index for assessing liquefaction hazard: lessons from historical data. Soils Found. **55**(4), 778–787 (2015). https://doi.org/10.1016/j.sandf.2015.06.010

McCloskey, J., Lange, D., Tilmann, F., Nalbant, S.S., Bell, A.F., Natawidjaja, D.H., Rietbrock, A.: The September 2009 Padang Earthquake. Nat. Geosci. **3**(2), 70–71 (2010). https://doi.org/10.1038/ngeo753

Nakamura, Y.: What is the Nakamura method? Seismol. Res. Lett. **90**(4), 1437–1443 (2019). https://doi.org/10.1785/0220180376

Newman, A.V., Hayes, G., Wei, Y., Convers, J.: The 25 October 2010 Mentawai tsunami earthquake, from real-time discriminants, finite-fault rupture, and tsunami excitation. Geophys. Res. Lett **38**(5), L05302 (2011). https://doi.org/10.1029/2010GL046498

Ntritsos, N., Cubrinovski, M.: A CPT-based effective stress analysis procedure for liquefaction assessment. Soil Dyn. Earthq. Eng. **131**, 106063 (2020). https://doi.org/10.1016/j.soildyn.2020.106063

Parihar, A., Anbazhagan, P.: Site response study and amplification factor for shallow bedrock sites. Indian Geotechnical Journal **50**, 726–738 (2020). https://doi.org/10.1007/s40098-020-00410-w

Porter, M., Lato, M., Quinn, P., Whittall, J.: Challenges with using risk matrices for geohazard risk management for resource development projects. In: MGR 2019: Proceedings of the First International Conference on Mining Geomechanical Risk. Australian Centre for Geomechanics, 9-11 April, Perth, Australia, pp. 71–84. (2019)

Putrie, N.S., Susiloningtyas, D., Pratami, M.: The distribution pattern of Settlements in 2032 was based on population density in Bengkulu City. IOP Conf. Ser.: Earth Environ. Sci. **284**(1), 012007 (2019). https://doi.org/10.1088/1755-1315/284/1/012007. (**IOP Publishing**)

Rafie, M.T., Sahara, D.P., Cummins, P.R., Triyoso, W., Widiyantoro, S.: Stress accumulation and earthquake activity on the Great Sumatran Fault. Indonesia. Natural Hazards **116**(3), 3401–3425 (2023). https://doi.org/10.1007/s11069-023-05816-2

Rahman, M.Z., Siddiqua, S., Kamal, A.M.: Liquefaction hazard mapping by liquefaction potential index for Dhaka City, Bangladesh. Eng. Geol. **188**, 137–147 (2015). https://doi.org/10.1016/j.enggeo.2015.01.012

Rai, A.K., Malakar, S., Goswami, S.: Active source zones and earthquake vulnerability around Sumatra subduction zone. J. Earth Syst. Sci. **132**(2), 66 (2023). https://doi.org/10.1007/s12040-023-02070-9

Riveros, G.A., Sadrekarimi, A.: Liquefaction resistance of Fraser River sand improved by a microbially-induced cementation. Soil Dyn. Earthq. Eng. **131**, 106034 (2020). https://doi.org/10.1016/j.soildyn.2020.106034

Seyedi-Viand, S.M., Eseller-Bayat, E.E.: Partial saturation as a liquefaction countermeasure: a review. Geotech. Geol. Eng. **40**, 499–530 (2022). https://doi.org/10.1007/s10706-021-01926-5

SNI 1726–2019.: Earthquake resistance planning procedures for building and non-building structures. National Agency of Standardisation, Jakarta: Indonesia. (2019)

Sonmez, H.: Modification of the liquefaction potential index and liquefaction susceptibility mapping for a liquefaction-prone area (Inegol, Turkey). Environ. Geol. **44**, 862–871 (2003). https://doi.org/10.1007/s00254-003-0831-0

Sonmez, H., Gokceoglu, C.: A liquefaction severity index suggested for engineering practice. Environ. Geol. **48**, 81–91 (2005). https://doi.org/10.1007/s00254-005-1263-9

Stewart, D., Knox, R.: What is the maximum depth liquefaction can occur?. Proceedings: Third International Conference on Recent Advances in Geotechnical Earthquake Engineering and Soil Dynamics. April 2–7, St. Louis, Missouri. (1995)

Sukkarak, R., Tanapalungkorn, W., Likitlersuang, S., Ueda, K.: Liquefaction analysis of sandy soil during strong earthquake in Northern Thailand. Soils Found. **61**(5), 1302–1318 (2021). https://doi.org/10.1016/j.sandf.2021.07.003

Swasdi, S., Chub-Uppakarn, T., Chompoorat, T., Sae-Long, W.: Numerical study on the influence of embedment footing and vertical load on lateral load sharing in piled raft foundations. Geomechanics and Engineering **36**(6), 545–561 (2024). https://doi.org/10.12989/gae.2024.36.6.545

Tjokrodimuljo, K.: Earthquake engineering. Gadjah Mada University, Yogyakarta, Indonesia, Department of Civil Engineering (2000)

Triyoso, W., Suwondo, A.: From the geodynamic aspect to earthquake potential hazard analysis of Liwa city and its surrounding. Nat. Hazards **116**(1), 1329–1344 (2023). https://doi.org/10.1007/s11069-022-05705-0

Vatresia, A., Utama, F.P., Sugianto, N., Widyastiti, A.: A hybrid deep learning and geoelectric sensing measurement over Bengkulu Flood. In: The 2023 IEEE 7th International Conference on Information Technology, Information Systems and Electrical Engineering (ICITISEE). IEEE. November 29-30, Purwokerto: Indoensia, pp. 100–105. (2023). https://doi.org/10.1109/ICITISEE58992.2023.10405208

Ventura, C.E., Finn, W.L., Onur, T., Blanquera, A., Rezai, M.: Regional seismic risk in British Columbia—classification of buildings and development of damage probability functions. Can. J. Civ. Eng. **32**(2), 372–387 (2005). https://doi.org/10.1139/l04-099

Vessia, G., Laurenzano, G., Pagliaroli, A., Pilz, M.: Seismic site response estimation for microzonation studies promoting the resilience of urban centers. Eng. Geol. **284**, 106031 (2021). https://doi.org/10.1016/j.enggeo.2021.106031

Wang, Y., Cao, T., Gao, Y., Shao, J.: Experimental study on liquefaction characteristics of saturated Yellow River silt under cycles loading. Soil Dyn. Earthq. Eng. **163**, 107457 (2022). https://doi.org/10.1016/j.soildyn.2022.107457

Wills, C.J., Gutierrez, C.I., Perez, F.G., Branum, D.M.: A next generation V_{S30} map for California based on geology and topography. Bull. Seismol. Soc. Am. **105**(6), 3083–3091 (2015). https://doi.org/10.1785/0120150105

Wood, H.O., Newman, F.: Modified Mercalli intensity of 1931. - Bull. Seismol. Soc. Amer. **21**, 277–283 (1931). https://doi.org/10.1785/BSSA0210040277

Yao, X., Qi, S., Liu, C., Guo, S., Huang, X., Xu, C., Zou, Y.: An empirical attenuation model of the peak ground acceleration (PGA) in the near field of a strong earthquake. Nat. Hazards **105**, 691–715 (2021). https://doi.org/10.1007/s11069-020-04332-x